ABSTRACT

Title of Thesis: PHASE BEHAVIOR AND INTERFACIAL PHENOMENA TERNARY SYSTEMS.

Deepa Subramanian, Master of Science, 2009

Directed By: Professor M.A. Anisimov –
Department of Chemical and Biomolecular Engineering
Institute for Physical Science and Technology

Co-Directed By: Professor R.A. Adomaitis –
Department of Chemical and Biomolecular Engineering
Institute for Systems Research

Phase behavior in multi-component systems has a wide variety of applications in the chemical process industry. In this work, the interfaces in two-phase, three-component systems were modeled and studied. Direct calculations of the asymmetric concentration profiles near the critical points of fluid phase separation are very difficult since they are affected by mesoscopic fluctuations. In this study a "complete scaling" approach was used to model interfacial profiles for a highly asymmetric, dilute ternary mixture near the critical point of liquid-liquid separation. The symmetric order parameter profile, the density profile of the lattice gas model, was used to further calculate the asymmetric interfacial concentration profiles at the mesoscale. Fluid asymmetry has been introduced through mixing of the physical field variables into the symmetric scaling theoretical fields. The system-dependent mixing coefficients were calculated from experimental data and a mean-field equation of state, namely, the Margules model. The resultant interfacial profiles for the concentration of water across the methanol-rich and cyclohexane-rich phases show the asymmetry associated with the contribution of the entropy into the symmetric order parameter profile.

PHASE BEHAVIOR AND INTERFACIAL PHENOMENA IN TERNARY SYSTEMS

By

Deepa Subramanian

Thesis submitted to the Faculty of the Graduate School of the
University of Maryland, College Park, in partial fulfillment
of the requirements for the degree of
Master of Science
2009

Advisory Committee:
Professor Mikhail A. Anisimov, Chair
Professor Jan V. Sengers
Professor Srinivasa R. Raghavan
Professor G. Sriram

Acknowledgements

I would like to thank my advisors, Dr. Anisimov and Dr. Adomaitis for all their help and support. I would also like to thank Dr. Sengers for his continuous guidance and advice throughout my research work.

I would also like to thank all the members of my research group for their help, and most importantly my family, for giving me an opportunity to further my education and knowledge.

List of Tables

List of Figures

Nomenclature

G^{id}	Ideal part of Gibbs energy
G^{E}	Excess part of Gibbs energy
$G = G^{\mathrm{mix}}$	Gibbs energy of mixture
x_i	Composition of species i, in mol fraction
T	Absolute temperature
R	Universal gas constant
Λ_{ij}	Binary interaction parameter in Wilson equation
λ_{ij}	Interaction energy between species i and j
v_i	Molar volume of i^{th} component
τ_{ij}	Binary interaction parameter in NRTL equation
Δg_{ij}	Characteristic energy between species i and j
$\boldsymbol{\alpha}$	Nonrandomness parameter
G^{E} (combinatorial)	Combinatorial part of excess Gibbs energy
G^{E} (residual)	Residual part of excess Gibbs energy
$\Phi_i, \theta_i, z_i, q_i$	UNIFAC parameters for i^{th} component
ΔP_{drop}	Pressure drop between inside and outside of a droplet/bubble
σ	Surface tension of planar interface
r	Radius of droplet/bubble
δ	Tolman length
A_{ij}	Binary interaction parameter in Margules approximation
C	Ternary interaction parameter in Margules approximation
μ_i	Chemical potential of species i
$\boldsymbol{a}_i$	Activity of species i
G_{ij}	Second derivative of G, with respect to components i and j
D	Determinant of second derivatives of G
D^*	Determinant of third derivatives of G
$D^{\#}$	Determinant of fourth derivatives of G
x_{ic}	Critical compoistion of component i

h_1	Ordering field
h_2	Thermal field
h_3	Dependent field, thermodynamic potential
μ_c	Critical chemical potential
T_c	Critical temperature
P_c	Critical pressure
$\Delta\hat{\mu}_i = \frac{\mu_i - \mu_{ic}}{k_B T_c}$	Reduced chemical potential of species *i*
$\Delta\hat{\mu}_{ij} = \frac{\mu_i - \mu_j}{k_B T_c}$	Reduced chemical potential between species *i* and *j*
$\Delta\hat{T} = \frac{T - T_c}{T_c}$	Reduced temperature
$\Delta\hat{P} = \frac{P - P_c}{k_B T_c}$	Reduced pressure
k_B	Boltzman constant
$\alpha = 0.11$	Universal critical exponent
$\beta = 0.326$	Universal critical exponent
$\nu = 0.623$	Universal critical exponent
$a_i,\ b_i,\ c_i$	System dependent constants
ϕ_1	Strongly fluctuating order parameter
ϕ_2	Weakly fluctuating order parameter
z	Height dependent co-ordinate
ε	Deviation from 4 dimensions
d	Number of dimensions
ξ	Half the width of interfacial thickness
ξ_0	Amplitude of corelation length
ρ	Density
ρ_c	Critical density
$\hat{\rho} = \frac{\rho}{\rho_c}$	Reduced density
S	Entropy
S_c	Critical entropy
$\hat{S} = \frac{S}{k_B}$	Reduced entropy
x	Composition of cyclohexane in mol fraction
x_{1c}	Critical composition of methanol in mol fraction
$x_{2c} = x_c$	Critical composition of cyclohexane in mol fraction
x_{3c}	Critical composition of water in mol fraction
x', x''	Composition of cyclohexane in two co-existing phases in mol fraction

D_0, D_1, D_2, B_0	System dependent constants, obtained from methanol-cyclohexane binary equilibrium data
a_{eff} , b_{eff}	Effective system dependent parameters, obtained from methanol-cyclohexane binary equilibrium data
A_0^-, B_{cr}	System dependent parameters for heat capacity
K	Krichevskii-type parameter
$\frac{d\hat{T}_c}{dx_3}$	Change in critical temperature of methanol-cyclohexane binary system, on the addition of water
$\frac{dx_1}{dx_3}$	Change in critical composition of methanol on the addition of water
$\frac{dx_2}{dx_3}$	Change in critical composition of cyclohexane on the addition of water
A_{12}^0	Margules parameter for methanol-cyclohexane binary system
A_{12}	Margules parameter for methanol-cyclohexane-water dilute ternary system

Table of Contents

Chapter 1: Introduction

In chemical engineering, mixtures are an integral part of everyday life. Multi-component fluids mixtures containing two, three or more components are present everywhere. Some of the common examples of multicomponent mixtures include – gasoline, used for automobiles which is a mixture of many aliphatic and some aromatic hydrocarbons, polymer blends which are used in making plastic materials like bags, bottles etc., biological cellular membranes which contain different chemical constituents like lipids, proteins and cholesterol, liquid based consumer products like detergents and shampoos which are a blend of surfactants, polymers and stabilizers.

The complex behavior of multicomponent mixtures makes them hard to understand. Multicomponent mixtures are also hard to model and their thermodynamics is not clearly understood. In this thesis, work has been done to understand the behavior of systems containing three-components, known as ternary systems. Interfacial behavior of three component fluids seen at the interface of two phases is also studied.

Some of the major applications in chemical engineering, such as reaction kinetics, liquid-liquid extraction, separation by distillation etc, all involve multi-phase systems. Most of the literature on multi-phase systems is obtained from experimental data.[2] The experimental work needed to predict higher order data is much larger than that needed for binary systems.[7] Hence, it may not always be possible to obtain experimental data for a particular system. Thus it becomes necessary and important to be able to model multi-phase systems.[1–4,7] In addition, experimental data for a particular system available in the literature may not always be sufficiently consistent or complete, to enable one to describe the entire system.[2,5-7] Due to these reasons, it is important to be able to theoretically model multi-phase systems. In the context of multi-phase systems, the work done here is based on understanding interfacial behavior of tree-component systems.

1.1 Interfacial phenomena

In mesoscopic systems, the interface separating two or more phases is not sharp, but rather smooth, and has a certain interfacial thickness associated with it.[11] Across this interface, there is a gradual change in the composition of the species. Such an interface is known as a smooth or hazy interface, as opposed to a sharp interface where the interfacial thickness is of the order of a molecule. A sharp interface is seen in fluids far away from the critical point, while a smooth interface is seen in fluids near the critical point.

For most real systems, the interface is asymmetric in nature and is affected by fluctuations, especially near the critical temperature. Determining the concentration profiles or density profiles across the interface, which include the effect of fluctuations, is not an easy task. Hence in this work, complete scaling[22,26,27] approach has been used to determine the concentration profiles in a highly asymmetric dilute ternary mixtures.

In the complete scaling approach, thermodynamic transformations are carried out between theoretical scaling variables and thermodynamic physical variables. A symmetric variable - the order parameter, density from the lattice gas model, is used to relate the theoretical scaling fields and the physical variables. Asymmetry is introduced through system dependent mixing coefficients. The mixing coefficients that depend on binary equilibrium data are determined by fitting experimental data to a scaled equation of state. The coefficients that depend on ternary equilibrium data are determined from a mean-field equation of state, such as Margules approximation. In addition to being able to model asymmetric interfacial concentration profiles, phase behavior in ternary systems is also analyzed. This is also done by using Margules approximation.

In this work, the use of Margules approximation model is two-fold. It is first used to describe phase behavior in ternary systems, which gave the author an idea on the role of the interactions parameters in the phase behavior of the ternary system. After understanding this, the model was then used in a novel way to determine the system

dependent coefficients needed to calculate the asymmetric interfacial concentration profiles.

1.2 Motivation to study interfacial behavior in asymmetric ternary systems

In order to contribute to the understanding of systems at the micro, meso and nano scales, it is important to understand smooth interfaces. This is because, when the thickness of the smooth interface between two phases is the order of a few nanometers, the distribution of components within the interface can be symmetric or asymmetric. In reference to this thesis, an asymmetric interface is described as an interface where there is a shift in the distribution of the dilute component between two rich phases. It has been shown[11] that an asymmetric behavior at the interface provides a significant contribution to a characteristic length, known as the Tolman length.

The Tolman length is a curvature correction to the surface tension. Tolman length is observed in nano-scaled droplets or bubbles which are at equilibrium between two phases. [12] Surface tension of a planar surface is described by the Young-Laplace equation as: $\Delta P_{\text{drop}} = \frac{2\sigma}{r}$, where ΔP_{drop} is the pressure drop between the inside and the outside of the droplet/bubble, r is the radius of the bubble/droplet and σ is the surface tension of the planar interface. For a tiny droplet, whose radius is the order of a few nanometers, it has been shown [12] that the surface tension is lower than that predicted by the Young-Laplace equation. Hence the Tolman length is defined as a correction to the surface tension of small curved objects. The corrected surface tension is defined as:

$\Delta P_{\text{drop}} = \frac{2\sigma}{r}\left(1 - \frac{\delta}{r}...\right)$, where δ is the Tolman length. This correction to surface tension has significant applications in chemical engineering. Some of the applications include[13] micro-porous flow, capillary action, wetting ability etc.

Recently, it has been shown[14] that the Tolman length is related to the asymmetry of the system. Interfacial thickness, related to the Tolman length,[11] is also described by using the concentration profiles developed at the interface.

1.3 Nature of phase behavior – symmetry vs. asymmetry

Phase behavior can be symmetric or asymmetric. In the context of this thesis, a symmetric system is described by the symmetric nature of its phase diagram, as shown in Fig. 1.1. A symmetric binary system has a phase diagram as shown below, where phase separation occurs at a concentration of 50%.

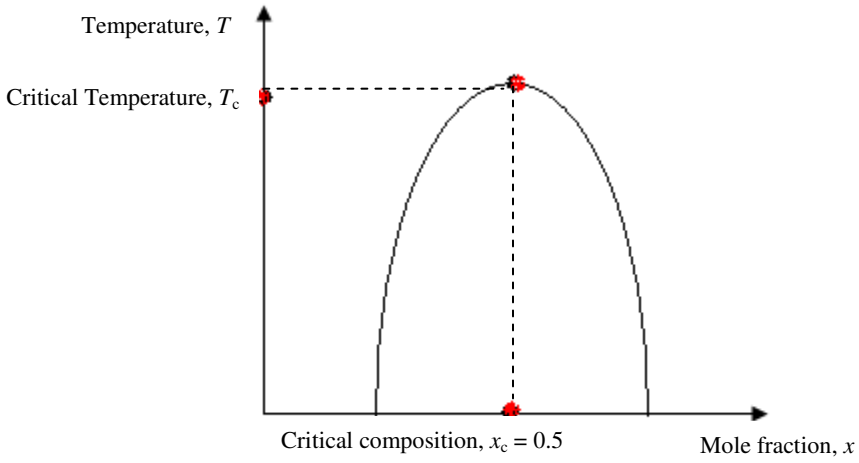

Fig. 1.1: A symmetric phase diagram observed in binary systems, where phase separation occurs at a critical composition of 0.5

As opposed to this, most ternary systems are asymmetric.[10] The phase separation in such ternary systems does not occur evenly, but each phase is rich in only one of the three phases. An example of such a ternary system is as shown in Fig. 1.2.

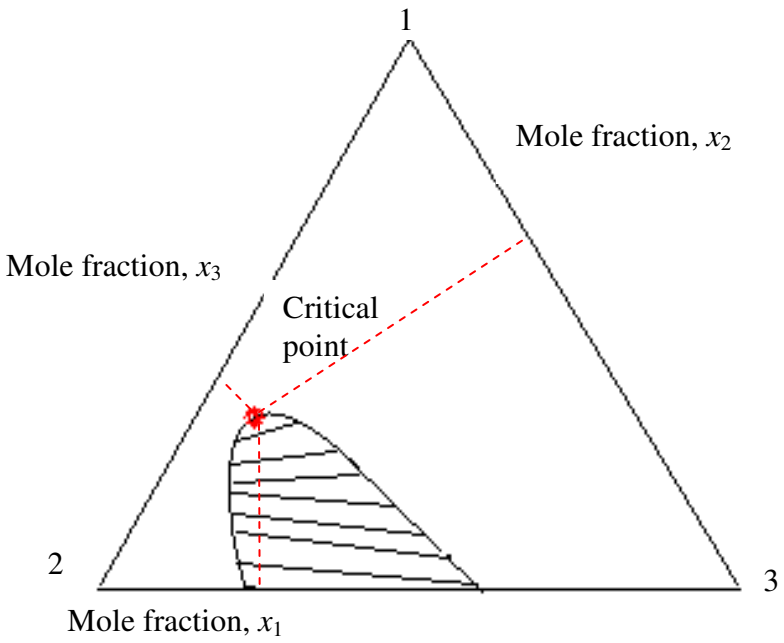

Fig. 1.2 An asymmetric ternary system, where phase separation at the critical point does not occur evenly.

In this work, focus has been on understanding how to model the asymmetry present at the interface of a dilute ternary fluid mixture.

1.4 Non-ideality in fluid mixtures

Margules approximation is a simple model that is used to determine the non-ideality in ternary systems. Margules approximation is chosen in this work, due to its simplicity. Some of the other models – mean filed equation of state are briefly described below.

Nonideality in fluid systems expressed through the excess Gibbs energy. In thermodynamics, Gibbs energy is defined as:

$$G = H - TS. \tag{1.1}$$

The excess Gibbs energy is then expressed as:

$$G^{\mathrm{E}} = H^{\mathrm{E}} - TS^{E}. \tag{1.2}$$

There are two main types of models used to predict the excess Gibbs energy. The simplest assumption is when S^E is assumed to be zero, and H^E is expressed as a function of mole fraction of the components and their interaction parameters, at constant temperature and pressure. Such a model is known as a regular solution model.[8] Another type of approach to predict the excess Gibbs energy is the athermal solution model which assumes H^E as zero.[8] Many models are available to describe the excess Gibbs energy in ternary systems. Some of the models include the Wilson equation, the Non-Random Two Liquid equation, the UNIQUAC method, Margules approximation etc.

1.5 Models for non-ideal systems

1.5.1 Wilson's equation

The Wilson equation,[3] used to predict excess Gibbs energy for systems with n components is:

$$\frac{G^E}{RT} = -\sum_{i=1}^{n} x_i \ln\left[\sum_{j=1}^{n} x_j \Lambda_{ij}\right] \tag{1.3}$$

where

$$\Lambda_{ij} \equiv \frac{v_j}{v_i} \exp\left[-\frac{\lambda_{ij} - \lambda_{ii}}{RT}\right]. \tag{1.4}$$

In the above expressions, x_i is the mole fraction of the i^{th} component, λ_{ij} is the interaction energy in Joule/mol between components i and j and v_i is the molar volume of the i^{th} component. As seen in the above equations, the calculations involve only binary data, without the need for ternary, quaternary or higher-order data. One disadvantage of the Wilson equation is that it cannot be used for systems containing partially miscible liquids.[7]

1.5.2 Non-random two-liquid model

Another model used to describe fluid phase equilibria in multi component systems is the NRTL or the non-random two liquid model developed by Rénon and

Prausnitz.[3,9] The NRTL model is applicable for more liquid mixtures and is not limited by partially miscible systems. The excess Gibbs energy predicted by the NRTL model is:

$$\frac{G^{\mathrm{E}}}{RT} = \sum_{i=1}^{n} x_i \frac{\sum_{j=1}^{n} \tau_{ji} G_{ji} x_j}{\sum_{l=1}^{n} G_{li} x_l} \tag{1.5}$$

where

$$\tau_{ji} = \frac{g_{ji} - g_{ii}}{RT}, \tag{1.6}$$

$$G_{ji} = \exp(-\alpha_{ji}\tau_{ji}), \text{ with } \alpha_{ji} = \alpha_{ij}. \tag{1.7}$$

In the above expressions, x_i is the mole fraction of the i^{th} component, Δg_{ij} is the characteristic energy in Joule/mol between components i and j and α_{ji} is a nonrandomness parameter. An advantage of the NRTL equation is that it can describe a wide variety of systems. However, it needs the specification of another parameter, α [9]

1.5.3 UNIQUAC model

Another model used to describe fluid phase equilibria is the UNIQUAC model, or the UNiversal QUAsiChemical model developed by Abrams and Prausnitz.[3,9] In the UNIQUAC model the excess Gibbs energy is represented as a sum of a 'combinatorial' excess Gibbs energy and a 'residual' excess Gibbs energy, as shown below:

$$\frac{G^{\mathrm{E}}}{RT} = \frac{G^{\mathrm{E}}(\text{combinatorial})}{RT} + \frac{G^{\mathrm{E}}(\text{residual})}{RT}, \tag{1.8}$$

$$\frac{G^{\mathrm{E}}(\text{combinatorial})}{RT} = \sum_{i=1}^{n} x_i \ln\frac{\Phi_i}{x_i} + \frac{z}{2}\sum_{i=1}^{n} q_i x_i \ln\frac{\theta_i}{\Phi_i}, \tag{1.9}$$

$$\frac{G^{\mathrm{E}}(\text{residual})}{RT} = -\sum_{i=1}^{n} q_i x_i \ln\left[\sum_{j=1}^{n} \theta_j \tau_{ji}\right]. \tag{1.10}$$

Where: $\tau_{ji} = \frac{g_{ji} - g_{ii}}{RT}$, $\Phi_i = \frac{r_i x_i}{\sum_{j=1}^{n} r_i x_i}$, $\theta_i = \frac{q_i x_i}{\sum_{j=1}^{n} q_i x_i}$.

In the above expressions, x_i is the mole fraction of the i^{th} component, r_i and q_i are molecular structure constants of the individual components.

The above calculations involve only binary data, without the need for ternary or higher-order data. The parameters can be estimated by using the UNIFAC method, where it is assumed that the functional groups, as opposed to entire molecules, are the main interacting species.[9] One disadvantage of describing fluid phase behavior by using the UNIQUAC model is the need to have an extensive set of accurate binary data readily available, which might be difficult.

The focus in this thesis is to be able to use a model that is not only simple to understand, but also flexible to apply. Hence, the Margules approximation for regular solutions is chosen to model ternary systems. For a three-component system, the Margules approximation consists of three binary-interaction parameters and a single ternary interaction parameter.[10] It is also applicable to more diverse systems and not limited by partial miscibility.[3]

This thesis consists of five chapters, starting with the introduction. In the second chapter modeling of ternary phases by using Margules approximation is described. The nature of the phase behavior – symmetric or asymmetric, is also analyzed. This analysis is further applied in chapter 3. In the third chapter scaling theory is discussed. An introduction to mesoscopic thermodynamics is also provided. Relations between theoretical scaling variables and thermodynamic physical variables are derived. System dependent coefficients, that relate the theoretical and physical variables, are also computed. A mean-field equation of state, the Margules approximation is used for this purpose. In the fourth chapter, the methanol-cyclohexane-water system is studied and analyzed by using the relations developed in chapter three. Interfacial concentration profiles for water are developed and plotted. Finally in the last chapter, the conclusions are summarized and future work is discussed.

Chapter 2: Modeling ternary systems

2.1 Introduction

In this chapter, ternary systems are modeled by using the Margules approximation. The basics for plotting and reading ternary diagrams on an equilateral triangle are explained first. Some of the different types of phase behavior observed in ternary systems are described next. The mathematical relations describing equilibrium in ternary systems are then evaluated. In this section, the Margules approximation is used to determine the excess Gibbs energy for three-component systems. The calculations for the binodal curve representing two-phase equilibrium, along with the spinodal curve, the limit of stability and the critical point, or the point of miscibility are presented. Results of the regular solution model, with varying values of the interaction parameter are discussed. The last section describes the basis for the choice of parameters in the Margules approximation.

2.2 Representing ternary systems on equilateral triangles

A triangular representation of a ternary system depicts the composition of each of the species in a three-component system. In a triangular plot, the sum of all the three species must be a constant value. Thus there are two unknown variables, and the third variable is fixed. In this thesis, the three species are designated as 1, 2 and 3, with 3 being the impurity in a mixture of 1 and 2. The amount of the three components is designated by mol fractions such as x_1, x_2 and x_3, where $x_1 = 1 - x_2 - x_3$.

- The triangles are plotted such that each vertex represents a pure species, or 100% of that component. *Example:* the vertex 1 contains only pure species 1.
- The altitude of the equilateral triangle from that vertex to the opposite base represents the % variation of the composition of the species. *Example:* the line 1-4 represents the % variation of species 1, from 100 % at 1 to 0 % at 4.

- The opposite base contains no amount of the species. *Example:* The line 2-3 contains the binary mixture 2 and 3 only.

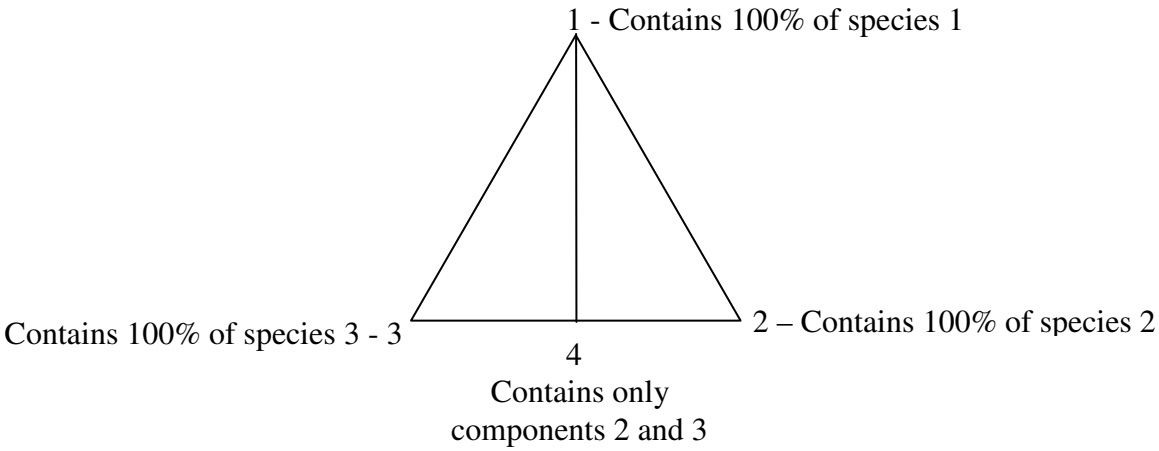

Fig. 2.1 Representation of pure species on triangular plots.

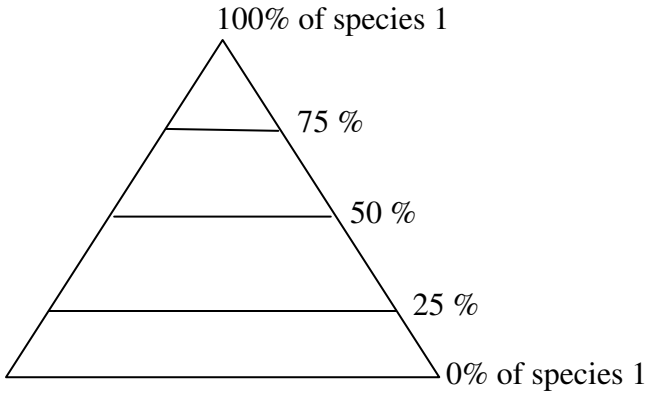

Fig. 2.2 Variation of composition of pure species 1.

- Any composition inside the triangle contains all the three species. *Example:* Point P contains all the three species1, 2 and 3 in varied proportions.

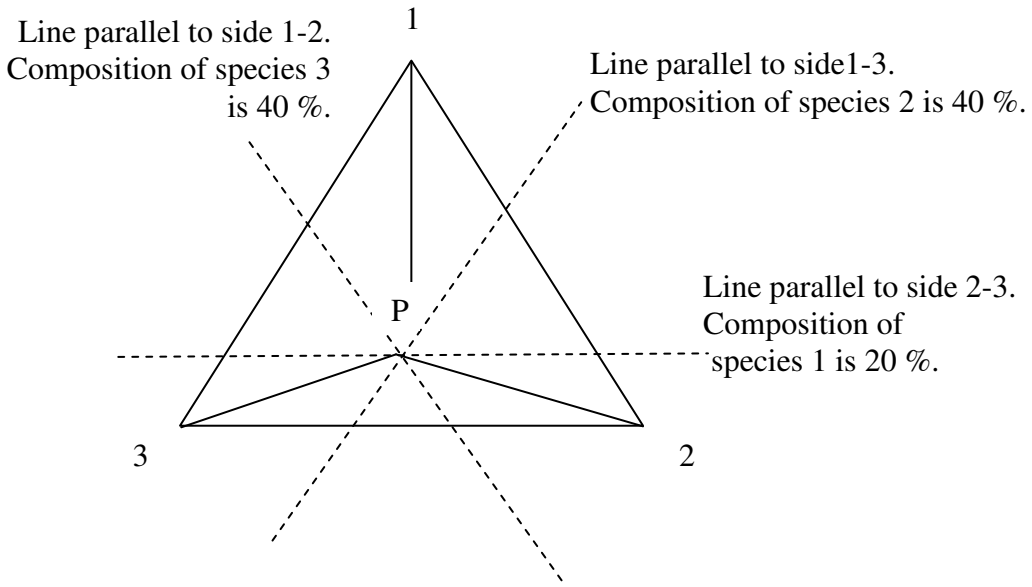

Fig. 2.3 Representation of a ternary composition P, within the triangular plot. Composition of point P is $x_1 = 20$ %, $x_2 = 40$ %, $x_3 = 40$ %.

2.3 Different phase behaviors seen in ternary systems

There exists a great variety of possible phase equilibria in ternary systems. The three basic types of ternary phase diagrams are described below.

2.3.1 Systems containing only two-phase regions

The equilibrium diagram of such systems looks like Fig. 2.4a. The figure shows one binary system which is heterogeneous.[10,17] It is one of the most frequently encountered systems.[1,10]

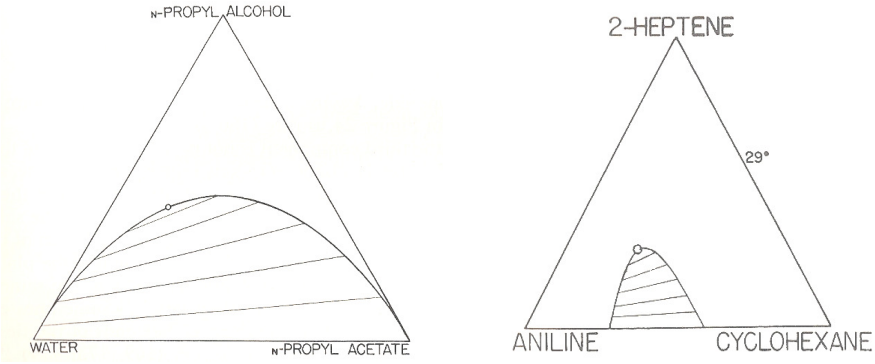

Fig. 2.4a Ternary systems with only one binary phase.[17]

If the system contains more than one heterogeneous binary system, the equilibrium curves look like Figs. 2.4b and 2.4c where there are two and three heterogeneous binary systems respectively.[10, 17]

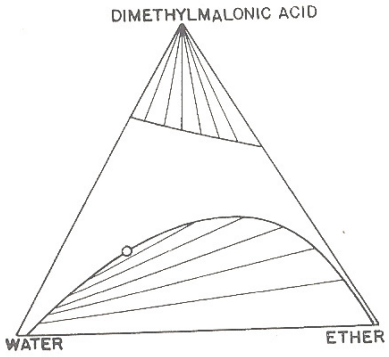

Fig. 2.4b Ternary system with two binary phases.[17]

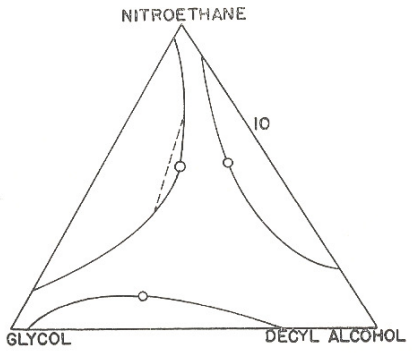

Fig. 2.4c Ternary system with three binary phases.[17]

2.3.2. Systems containing multiple-phase regions

A basic type of a ternary system exhibiting a multiple-phase region is shown in Fig. 2.5. [10, 17]

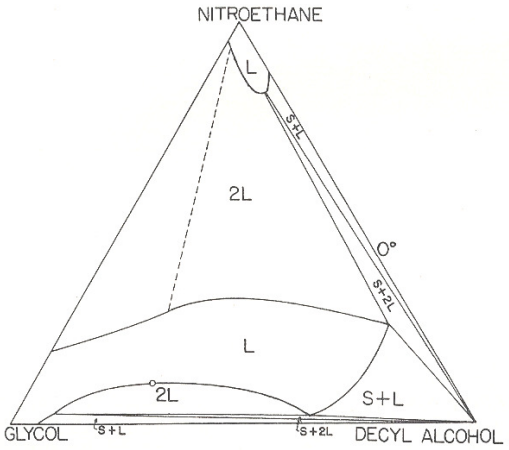

Fig.2.5 Formation of multiple-phase regions by superposition of various two-phase regions.[17]

Such systems are rarely found experimentally.[10]

2.3.3. Systems with closed miscibility region (island curve)

Systems with a closed miscibility region appear as shown in Fig. 2.6. An island is formed when one of the binary systems shows high negative deviations from Raoult's Law, while the other binary systems are homogeneous with identical positive deviations from Raoult's law. Island curves can also be formed when there are strong interactions among all the three components of the system, which can even be interpreted as the formation of an additional component.[10]

Example: Water, Acetone, Phenol[10, 17]

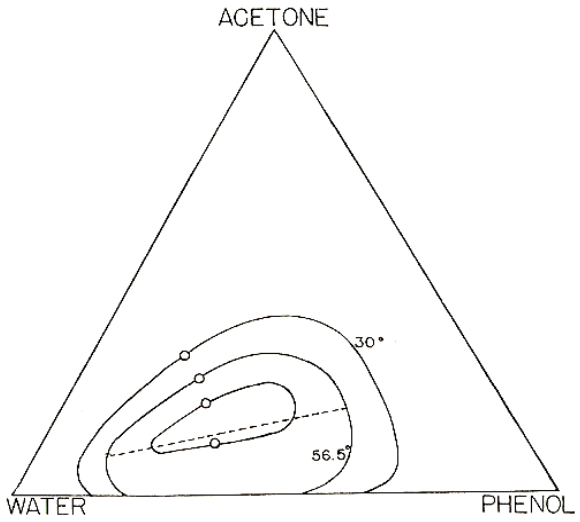

Fig. 2.6 Ternary system exhibiting a closed loop solubility curve.[10,17]

2.4 Effect of Temperature and Pressure

The systems represented on triangular plots are under conditions of constant temperature and pressure. Temperature can play a critical role in the nature of the phase diagram for ternary systems, especially in the vicinity of the critical temperature.

As an example, let us consider the water-phenol-acetone system. At temperatures below 65 ºC, the curve corresponds to Fig 2.4a, and above 65 ºC the curve corresponds to a closed loop solubility curve as seen in Fig. 2.6.[10, 17]

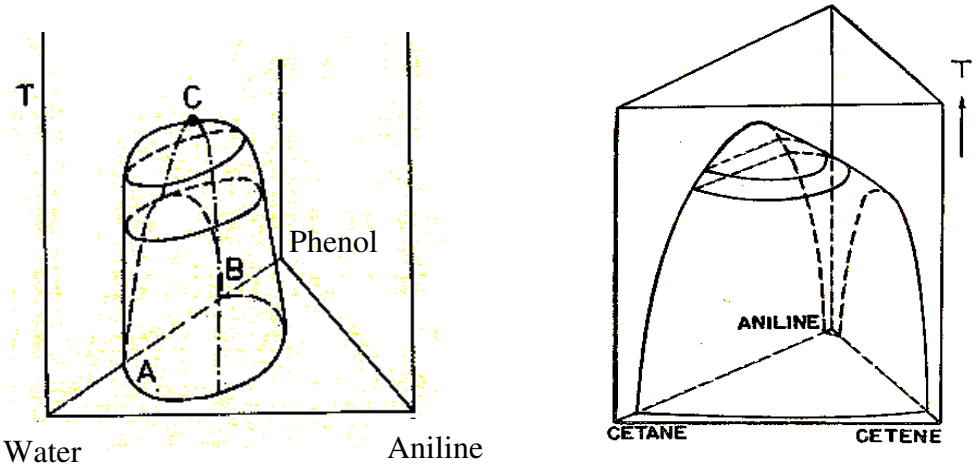

Fig. 2.7 Effect of temperature on ternary systems [10,17]

In the current work, a regular solution model under isothermal-isobaric condition is simulated to describe systems as shown in Fig. 2.4a, where there is a single heterogeneous binary system.

2.5 Regular solution model – Margules approximation

As described earlier in chapter 1, many methods such as Wilson's equations, NRTL, UNIQUAC are available to model multi-component systems. In this section a strictly regular solution for ternary systems is modeled by using the Margules approximation.

In this model the excess Gibbs energy $\frac{G^{E}}{RT}$ is expressed as:[4, 9,10]

$$\frac{G^{E}}{RT} = A_{12}x_1x_2 + A_{23}x_2x_3 + A_{13}x_1x_3 + Cx_1x_2x_3 ,$$

where A_{ij} is the binary interaction parameter between components i and j, and depend on temperature T, and pressure P, only. The variables x_1, x_2 and x_3 are the mole fractions of the individual components present in the ternary system. C is a ternary constant and depends on the interactions between all the three components. The ideal Gibbs energy for a system is given as:

$\frac{G^{id}}{RT} = x_1 \ln x_1 + x_2 \ln x_2 + x_3 \ln x_3$. Thus the Gibbs energy of a ternary mixture is:

$$\frac{G^{mix}}{RT} = x_1 \ln x_1 + x_2 \ln x_2 + x_3 \ln x_3 + A_{12}x_1x_2 + A_{23}x_2x_3 + A_{13}x_1x_3 + Cx_1x_2x_3 .$$

For simplicity we will ignore the effects of C, and study the equilibrium behavior based only on the binary interaction parameters. Hence, for the purpose of this thesis:

$$G = \frac{G^{mix}}{RT} = x_1 \ln x_1 + x_2 \ln x_2 + x_3 \ln x_3 + A_{12}x_1x_2 + A_{23}x_2x_3 + A_{13}x_1x_3. \quad (2.1)$$

2.6 Conditions for thermodynamic stability

2.6.1. Determination of the equilibrium curve – Binodal

The binodal curve in a ternary system discussed here is a two-phase, three-component system. Initially, there exists a binary mixture of components 1 and 2, to which an impure component 3 has been added. As a result component 3 causes components 1 and 2 to separate into two phases. Each phase contains all the three components, but in varying proportions. Under the conditions of thermodynamic equilibrium, both the phases will be in equilibrium. As a result, the chemical potential of each component in the first phase will be equal to the chemical potential of the same component in the second phase.[9,10,15]

$$\begin{aligned} \mu_1^{'} &= \mu_1^{''} \\ \mu_2^{'} &= \mu_2^{''} \\ \mu_3^{'} &= \mu_3^{''}. \end{aligned} \tag{2.2}$$

The chemical potential here is the first derivative of Gibbs energy $\mu_1 = \frac{\partial G}{\partial x_1}$. It is expressed as logarithm activity: $\mu_1 = \ln \boldsymbol{a}_1$. Therefore we have:

$$\begin{aligned} \boldsymbol{a}_1^{'} &= \boldsymbol{a}_1^{''} \\ \boldsymbol{a}_2^{'} &= \boldsymbol{a}_2^{''} \\ \boldsymbol{a}_3^{'} &= \boldsymbol{a}_3^{''}. \end{aligned} \tag{2.3}$$

Hence in order to determine the binodal curve, the above set of three equations, Eq. (2.3) containing four variables – namely $x_1^{'}, x_2^{'}, x_1^{''}$ and $x_2^{''}$ (x_3 is a dependent variable obtained as $x_3 = 1 - x_1 - x_2$) are solved simultaneously.

2.6.2 Determination of the limit of stability - Spinodal

For multi-component systems, the generic criterion for thermodynamic stability at constant temperature T and pressure P is expressed as:[9,10]

$$D = \begin{vmatrix} G11 & G12 \ldots\ldots\ldots\ldots & G1(N-1) \\ G12 & G22 \ldots\ldots\ldots\ldots & G2(N-1) \\ \vdots & \vdots & \vdots \\ G1(N-1) & G2(N-1) \ldots\ldots & G(N-1)(N-1) \end{vmatrix} \geq 0, \quad (2.4)$$

where, G_{ij} is the second derivative of G, with respect to x_i and x_j, where the number of components of the system are *1* to *N*.

At the limit of stability, i.e. at the spinodal condition, $D = 0$. For a three-component system with $N = 3$, the above condition reduces to:

$$D = G11.G22 - (G12)^2 = 0, \quad (2.5)$$

$$G11 > 0,\ G22 > 0.$$

The above Eq. (2.5) is solved to determine the spinodal curve.

2.6.3 Determination of the critical point

At the critical point, where the Binodal merges with the Spinodal, additional conditions need to be satisfied which are given as:[4,9,10]

$$D^{*}=\begin{vmatrix} \dfrac{\partial D}{\partial x_1} & \dfrac{\partial D}{\partial x_2} & \cdots\cdots\cdots & \dfrac{\partial D}{\partial x_{N-1}} \\ G12 & G22 & \cdots\cdots & G2(N-1) \\ \vdots & \vdots & & \vdots \\ G1(N-1) & G2(N-1) & G(N-1)(N-1) & \end{vmatrix} \geq 0,$$

$$D^{\#}=\begin{vmatrix} \dfrac{\partial D^{*}}{\partial x_1} & \dfrac{\partial D^{*}}{\partial x_2} & \cdots\cdots\cdots & \dfrac{\partial D^{*}}{\partial x_{N-1}} \\ G12 & G22 & \cdots\cdots & G2(N-1) \\ \vdots & \vdots & & \vdots \\ G1(N-1) & G2(N-1) & G(N-1)(N-1) & \end{vmatrix} \geq 0.$$

For ternary systems these are reduced to:

$$D^{*}=\left(\frac{\partial D}{\partial x_1}\right).G22-\left(\frac{\partial D}{\partial x_1}\right).G12=0, \tag{2.6}$$

$$D^{\#}=\left(\frac{\partial D^{*}}{\partial x_1}\right).G22-\left(\frac{\partial D^{*}}{\partial x_1}\right).G12 \;\geq\; 0. \tag{2.7}$$

The equality in Eq. (2.6) is solved to obtain the critical point.

2.7 Modeling of two-phase ternary systems using Margules approximation

In the following section, two-phase three-component systems are described by using the relations developed in the above analysis. The nature of the phase behavior of ternary systems is studied with respect to the variation of the binary interaction parameters in Margules approximation Eq. (2.1). The binodal, spinodal and the critical point are determined as per Eqs. (2.3), (2.5) and (2.6) respectively.

2.7.1 Formation of 2 phases with parameters A_{12}, A_{23}, A_{13} all distinct:

Example 1: A_{12} =1.0 A_{23} = 0.5 A_{13} = 3.0

The critical composition is x_1 = 0.385 x_2 = 0.340 x_3 = 0.275.

The resultant ternary phase diagram is as shown in Fig. 2.8.

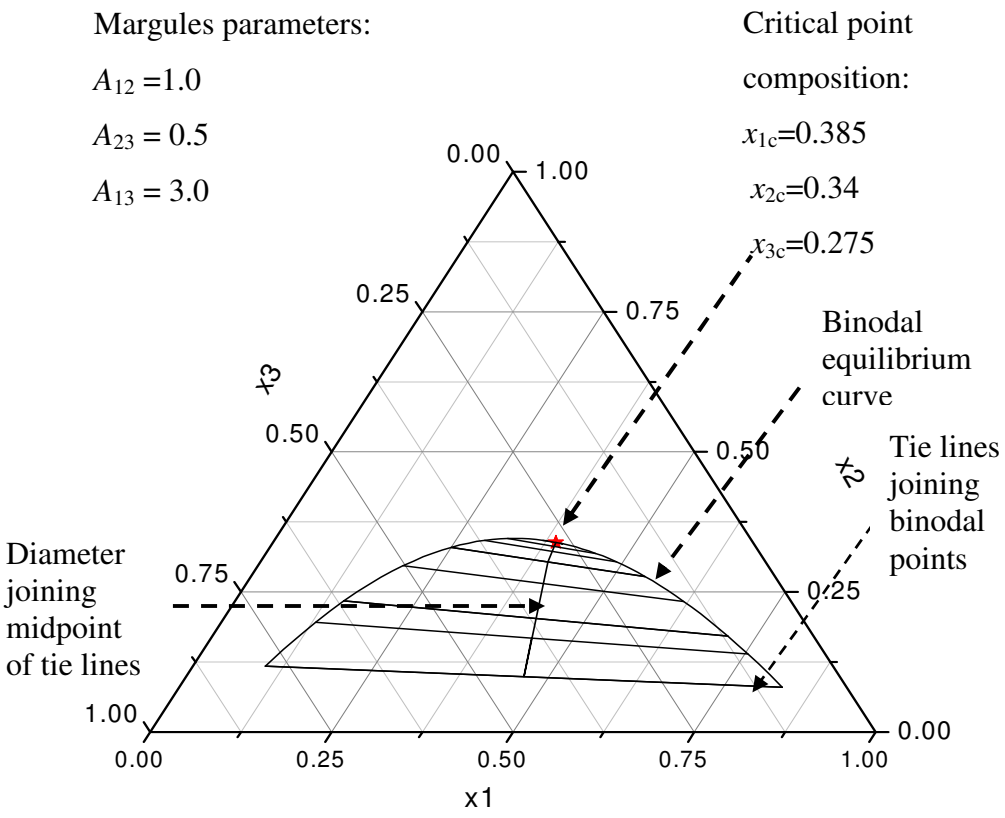

Fig. 2.8 Asymmetric ternary system with Margules parameters as: A_{12} =1.0, A_{23} = 0.5, A_{13} = 3.0.

Example 2: A_{12} =1.0 A_{23} = 1.5 A_{13} = 3.0

The critical composition is $x_1 = 0.240$ $x_2 = 0.340$ $x_3 = 0.420$.

The resultant ternary phase diagram is as shown in Fig. 2.9.

Margules parameters:

A_{12} =1.0

A_{23} = 1.5

A_{13} = 3.0

Critical composition:

x_1=0.240

x_2=0.340

x_3=0.420

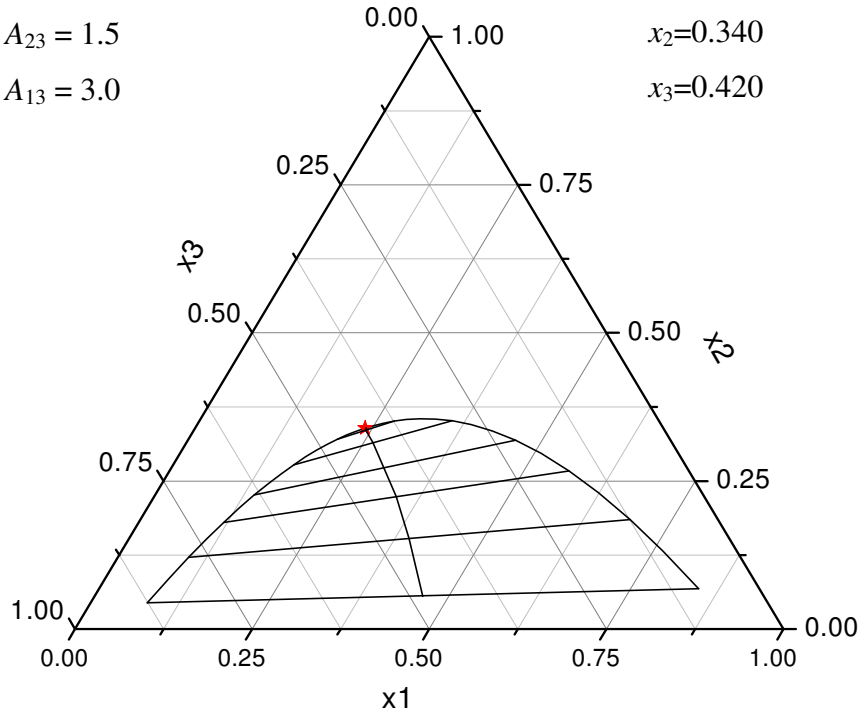

Fig. 2.9 Asymmetric ternary system with Margules parameters as:
A_{12} =1.0, A_{23} = 1.5, A_{13} = 3.0

Observations:

The tie lines are not parallel to each other, and the critical point is towards one side of the phase diagram. The rectilinear diameter (the line joining the mid points of the tie lines) is curved. This is the most commonly observed equilibrium diagram, and many ternary systems follow this. This is considered the ***asymmetric case***, due to the un-parallel nature of the lines, and the curved nature of the rectilinear diameter (as seen in the triangular diagram).

2.7.2 Formation of 2 phases with parameters $A_{12} = A_{23} = A$ and A_{13} distinct:

Example 1: $A_{12} = 1.0$ $A_{23} = 1.0$ $A_{13} = 3.0$

The critical composition is $x_1 = 0.333$ $x_2 = 0.333$ $x_3 = 0.333$.

The resultant ternary phase diagram is as shown in fig. 2.10

Margules parameters:

$A_{12} = 1.0$

$A_{23} = 1.0$

$A_{13} = 3.0$

Critical composition:

x_1=0.333

x_2=0.333

x_3=0.333

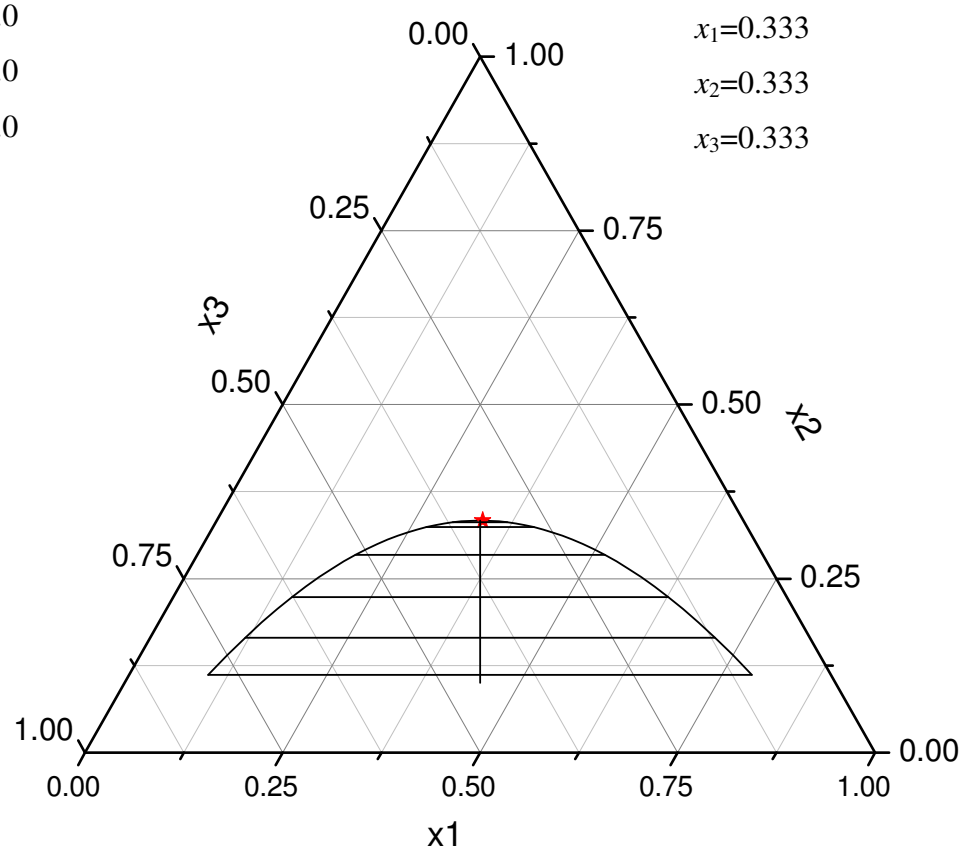

Fig. 2.10 Symmetric ternary system with Margules parameters as:
$A_{12} = 1.0$, $A_{23} = 1.0$, $A_{13} = 3.0$

Example 2: $A_{12} = 2.0$ $A_{23} = 2.0$ $A_{13} = 2.5$

The critical composition is $x_1 = 0.400$ $x_2 = 0.200$ $x_3 = 0.400$

The resultant ternary phase diagram is as shown in Fig. 2.11

Margules parameters:

$A_{12} = 2.0$

$A_{23} = 2.0$

$A_{13} = 2.5$

Critical composition

$x_1 = 0.400$

$x_2 = 0.200$

$x_3 = 0.400$

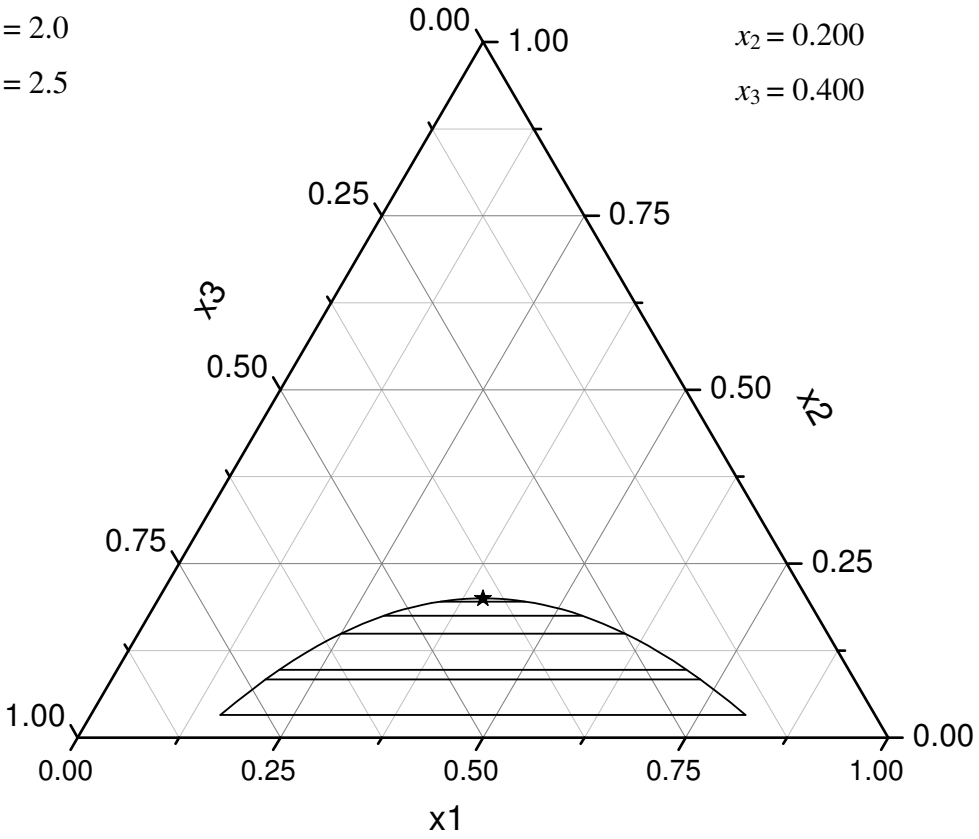

Fig. 2.11 Symmetric ternary system with Margules parameters as: $A_{12} = 2.0$, $A_{23} = 2.0$, $A_{13} = 2.5$.

Example 3: A_{12} =0.0 A_{23} = 0.0 A_{13} = 3.0

The critical composition is x_1=0.333 x_2=0.333 x_3=0.333.

The resultant ternary phase diagram is as shown in Fig. 2.12.

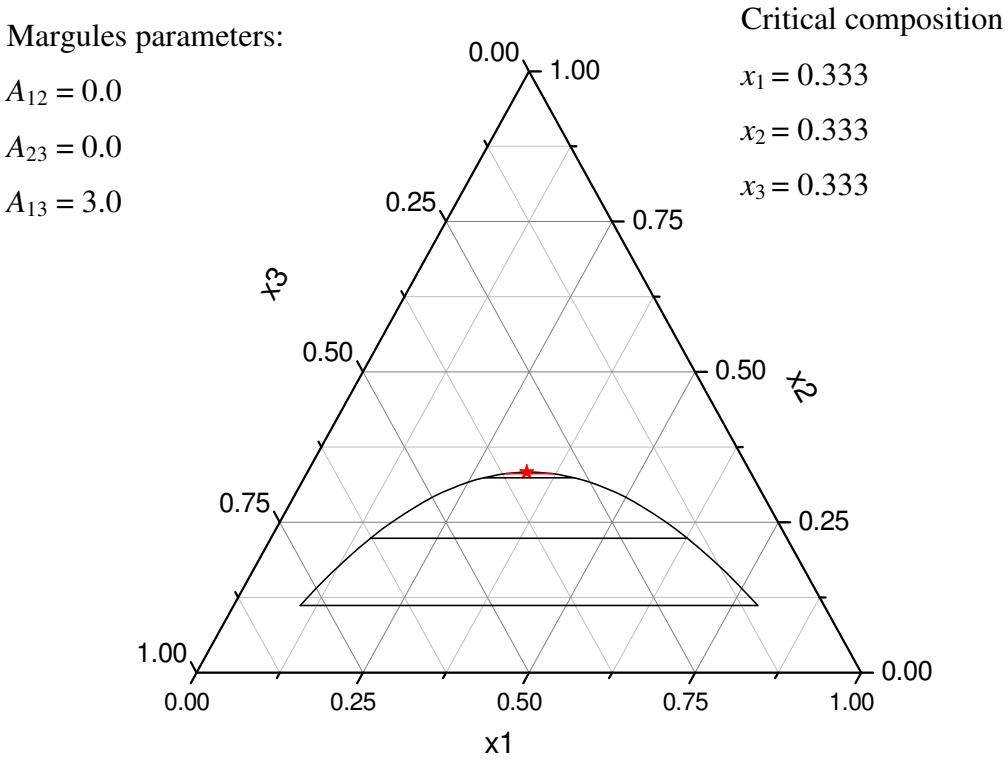

Fig. 2.12 Symmetric ternary system with Margules parameters as: A_{12} = 0.0, A_{23} = 0.0, A_{13} = 3.0

Observations:

As observed in these figures, the tie lines are parallel to each other, and the critical point is on top of the phase diagram. The rectilinear diameter is a straight line, perpendicular to the base. This case can be considered as the symmetric case, as the rectilinear diameter is a straight line and perpendicular to the base of the equilateral triangle.

Another observation made here, is that the critical phase separation in both the above examples occurs when: x_1= x_3= (1 - x_2)/2. Therefore the system can be considered symmetric with respect to x_1 and x_3.

2.8 Choice of parameters in Margules approximation for symmetric phase behavior

2.8.1 $A_{12} = A_{23} = 0.0$ and A_{13} distinct

From the above observations, critical composition occurs at $x_1 = x_3 = (1 - x_2)/2$.

Eq. (2.5) for the Spinodal reduces to:

$D = [-A_{13}^2\, x\, (1-x)^2 - 2A_{13}\, (1-x)^2 + 4]/[x(1-x)^2]$, where $x = x_2$. This equation is nonlinear in x and quadratic in A_{13}. Solving for A_{13} we obtain:

$A_{13}\,(1) = 2/(1-x)$

$A_{13}\,(2) = -2/(x\,(1-x))$

Therefore for different values of x (= x_2), when we determine A_{13}, we observe that:

$A_{13} > 2.0$ or $A_{13} < -8.0$. Intermediate values in between will give no phase separation.

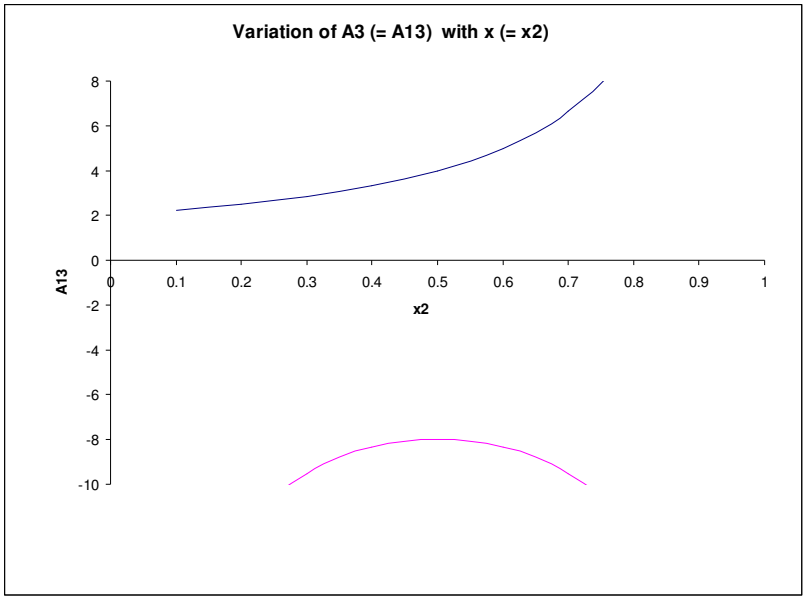

Fig. 2.13 Variation of interaction parameter A_{13} with variation in composition of species 2.

Notice when $A_{13} > 2.0$, the ternary phase diagram observed will be similar to those in Figs. 2.8, 2.9 and 2.10. (symmetric case with parallel tie lines). When $A_{13} < -8.0$, the ternary phase diagram obtained is a closed curve (not modeled yet) as seen in Fig. 2.6.

2.8.2 $A_{12} = A_{23} = A$ and A_{13} distinct:

Similar to above analysis, at the spinodal condition there are two values for the interaction parameter A_{13} as follows:

A_{13} (1) = 2/(1-x)

A_{13} (2) = 4A - 2/(x(1-x))

Therefore for different values of x (= x_2) and different values of A (=A_{12}=A_{23}), A_{13} is determined as shown below:

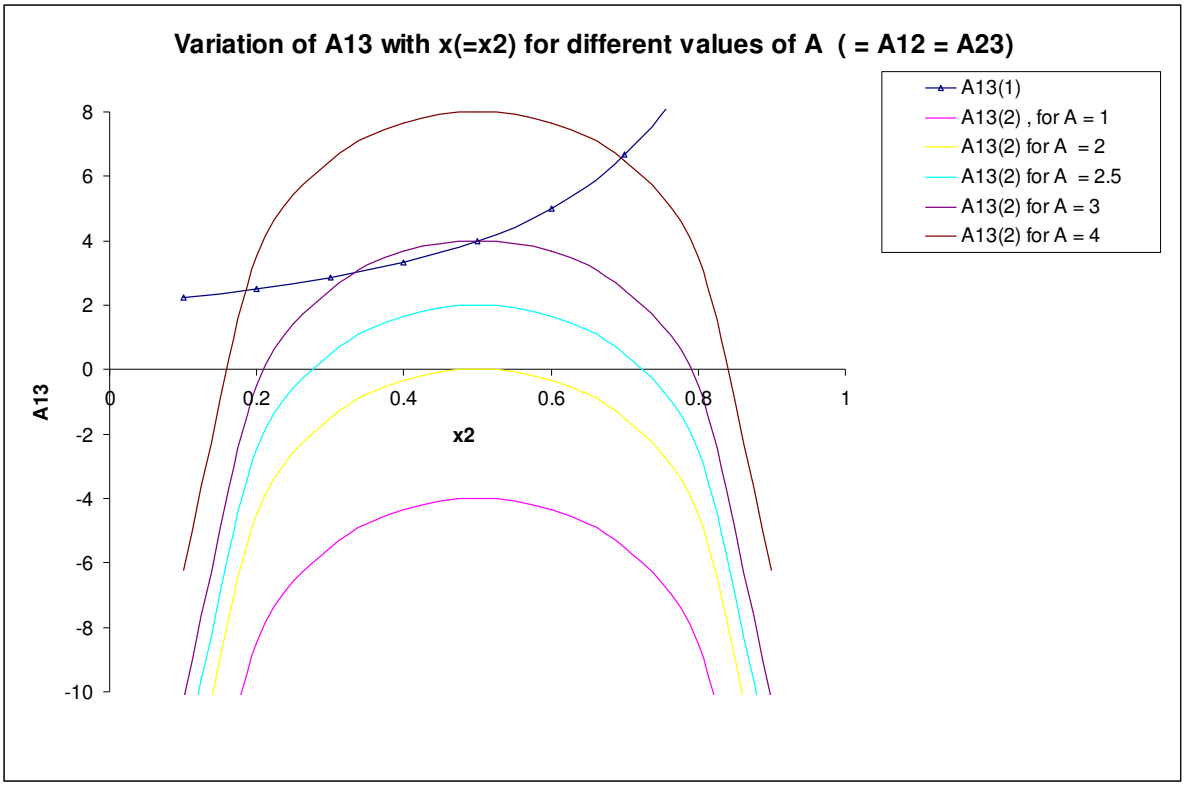

Fig. 2.14 Variation of interaction parameter A_{13} with variation in other interaction parameter A (where $A = A_{12} = A_{23}$).

The heterogeneous region is within the parabolic curve and above the non-linear polynomial curve. Between them is the homogeneous region, where no phase separation is seen.

Chapter 3: Interfacial Behavior

3.1 Interfaces

As discussed earlier in chapter 1, to understand systems at the micro, meso and nano scales, it is important to understand smooth interfaces. A smooth interface exists when there is a gradual change in the concentration of the species at the interface between two phases. Smooth interfacial concentration profiles are seen in near-critical binary systems, as well as in polymer solutions and polymer blends.[11,14] Smooth interfaces are observed in systems where the interfacial thickness is the order of a few nanometers and/or has a curved interface.[11,12] In addition, the surface tension of a curved interface is different than that of a planar interface.[11-14] Hence, in this thesis, work has been done to understand how the surface tension of a curved interface is related to important physical properties such as the thickness of the interface[11-14] and the asymmetric nature of the interface.[11,14]

In this thesis, interfacial concentration profiles for ternary systems are developed. Specifically, in a three-component, two-phase system, the gradual change in the composition of the dilute third species at the interface between two phases is determined. To determine this concentration profile, concepts from mesoscopic thermodynamics are employed.

3.2 Introduction to mesoscopic thermodynamics

In mesoscopic thermodynamics, a new length scale, larger than the atomistic scale and smaller than the macroscopic scale, becomes significant.[13] This new length is associated with the structure of materials and includes thermal fluctuations which arise due to the random thermal motion of particles from their average equilibrium values.[13] Fluctuations are important near second-order phase transitions in liquids and liquid mixtures.[13,18] A second-order phase transition is characterized by a divergence in properties such as the specific heat, isothermal compressibility, magnetic susceptibility

etc. Examples of the second-order phase transition include glass transition, critical phase transition, magnetism etc.

Close to the critical point, all physical properties obey simple scaling laws.[13,18] The scaling powers are universal in nature and are characterized by *critical exponents*. The theory that explains these power laws is known as *scaling theory*. The theory that calculates the values of these universal critical exponents is known as *renormalization-group theory*. The principle that governs the nature of critical phenomena is called *critical point universality*. The physical parameter that governs this scaling theory is the mesoscopic characteristic length, known as the *correlation length*, ξ, or the spatial extent of the fluctuations of an appropriate order parameter.[13]

3.3 Definition of order parameter

The concept of an order parameter, first introduced by Landau,[19] is used to describe the change in the structure of a system when it goes through a phase transition.[19] The order parameter is defined as a certain property, which varies from system to system. It has a zero value in the disordered phase above the critical point, and a finite value in the ordered phase below the critical point.[13,18,19] Critical points can exist between two phases only when they have an internal symmetry between them. For example solids have a unit cell or a crystal as part of their internal symmetry which is absent in liquids and gases. There can be no critical point between two phases that have a different internal symmetry and their coexistence curve either continues to infinity or intersects with another coexistence curve. [13,18,19]

3.4 Universality of critical behavior – Scaling theory

Different models are used to describe phase transitions– such as the Ising model or the mean-field model. Each model has a different set of critical indices associated with it to describe a phase transition such as the critical point. Phase transitions which are described by using the same set of critical indices are said to belong to the same

universality class.[18] An example of critical point universality is the description of various fluids and fluid-mixtures, which all belong to the 3-dimensional Ising model.[20] This behavior is described by using the scaling theory, with scaling laws, universal exponents and system-dependent amplitudes which have the same critical amplitude ratios.[20] Thus, in order to describe the thermodynamic behavior of a fluid near the critical point, scaling theory is used.[21]

Scaling theory includes theoretical variables, which are related to the physical properties of the system. The theoretical variables include two independent theoretical scaling fields, h_1 (ordering field) and h_2 (thermal field). By using the complete scaling approach, [22] the scaling fields for a pure fluid are defined as:

$$h_1 = a_1\Delta\hat{\mu} + a_2\Delta\hat{T} + a_3\Delta\hat{P}, \qquad (3.1)$$
$$h_2 = b_1\Delta\hat{T} + b_2\Delta\hat{\mu} + b_3\Delta\hat{P},$$

where a_i and b_i are system dependent constants and the reduced thermodynamic properties are defined as:

$$\Delta\hat{\mu} = \frac{\mu - \mu_c}{k_B T_c},$$
$$\Delta\hat{T} = \frac{T - T_c}{T_c},$$
$$\Delta\hat{P} = \frac{P - P_c}{P_c},$$

where k_B is the Boltzman's constant, T_c is the critical temperature, P_c is the critical pressure and μ_c is the critical chemical potential of the pure fluid.

A third field h_3, depends on the two scaling fields h_1 and h_2 as:

$$h_3 = |h_2|^{2-\alpha} f^{\pm}\left(\frac{h_1}{|h_2|^{2-\alpha-\beta}}\right), \qquad (3.2)$$

where $f^{\pm}$ is a scaling function and the superscript $\pm$ refers to the positive thermal field $h_2 > 0$ and the negative thermal field $h_2 < 0$ respectively.[23] The above equation

contains two system-dependent amplitudes $f^{\pm}$ and two universal critical exponents α and β. The dependent scaling field h_3 is related to the physical properties as:

$$h_3 = c_1 \Delta \hat{P} + c_2 \Delta \hat{\mu}_1 + c_3 \Delta \hat{T}. \tag{3.3}$$

The other theoretical variables are the theoretical scaling densities – the strongly fluctuating order parameter ϕ_1 and the weakly fluctuating order parameter ϕ_2. The scaling fields and the scaling densities are related as: [23]

$$dh_3 = \phi_1 dh_1 + \phi_2 dh_2 . \tag{3.4}$$

3.5 Principle of isomorphism

The scaling theory, used to describe critical phenomena, is universal with respect to the critical exponents.[20] As mentioned above, all fluids and fluid mixtures belong to the 3-dimensional Ising universality class. This means that the order parameter, previously defined, is either a scalar or a one-component vector.[18-21,23] The order parameter is such that the universal critical behavior is symmetric with respect to the order parameter.[19] The order parameter is a symmetric theoretical variable and for real liquid systems, it is related to a physical property like the density.[18-20] Hence, the physical thermodynamic variables which are asymmetric in nature are transformed into the theoretical space in order to determine their asymmetry. The asymmetric behavior of the system arises from the relations between the theoretical variables and the physical variables as defined in Eqs. (3.1-3.3). These equations are defined for one component fluids. The extension of the critical point universality to binary and ternary systems in order to depict the asymmetric nature of phase transition is known as isomorphism of critical phenomena.[24 - 26] Accordingly, the scaling fields for ternary systems are:

$$\begin{aligned} h_1 &= a_1 \Delta \hat{\mu}_1 + a_2 \Delta \hat{T} + a_3 \Delta \hat{P} + a_4 \Delta \hat{\mu}_{21} + a_5 \Delta \hat{\mu}_{31}, \\ h_2 &= b_1 \Delta \hat{T} + b_2 \Delta \hat{\mu}_1 + b_3 \Delta \hat{P} + b_4 \Delta \hat{\mu}_{21} + b_5 \Delta \hat{\mu}_{31}, \\ h_3 &= c_1 \Delta \hat{P} + c_2 \Delta \hat{\mu}_1 + c_3 \Delta \hat{T} + c_4 \Delta \hat{\mu}_{21} + c_5 \Delta \hat{\mu}_{31}, \end{aligned} \tag{3.5}$$

where

$$\Delta\hat{\mu}_{ji} = \frac{\mu_j - \mu_i}{k_B T_c},$$

a_i, b_i and c_i are system dependent constants. For a ternary system the system dependent amplitudes for the scaling fields h_1 and h_2, as defined by Eq.(3.2) are a_4 and b_1 respectively.[23,25] This comes from the fact that, under the "incomplete" scaling approach, the scaling fields were defined as:[21]

$$h_1 = \Delta\hat{\mu},$$
$$h_2 = \Delta\hat{T}.$$

Thus the three scaling fields for a ternary system are:

$$\begin{aligned} h_1 &= \Delta\hat{\mu}_{21} + a_1\Delta\hat{\mu}_1 + a_2\Delta\hat{T} + a_3\Delta\hat{P} + a_5\Delta\hat{\mu}_{31}, \\ h_2 &= \Delta\hat{T} + b_2\Delta\hat{\mu}_1 + b_3\Delta\hat{P} + b_4\Delta\hat{\mu}_{21} + b_5\Delta\hat{\mu}_{31}, \\ h_3 &= c_1\Delta\hat{P} + c_2\Delta\hat{\mu}_1 + c_3\Delta\hat{T} + c_4\Delta\hat{\mu}_{21} + c_5\Delta\hat{\mu}_{31}. \end{aligned} \tag{3.6}$$

3.6 Physical fields and physical variables

For a ternary system, the scaling fields are defined in Eq. (3.6). These equations relate the theoretical scaling fields to the physical properties. It is now important to derive expressions for the thermodynamic physical variables from the Gibbs-Duhem relation. The Gibbs-Duhem relation for *i* components is given as:

$$\Sigma x_i d\mu_i - \left(\frac{\partial\mu}{\partial T}\right)_{P,x} dT - \left(\frac{\partial\mu}{\partial P}\right)_{T,x} dP = 0.$$

For a three-component system, the Gibbs-Duhem equation becomes:

$$(1-x_2-x_3)d\mu_1 + x_2 d\mu_2 + x_3 d\mu_3 - \left(\frac{\partial \mu}{\partial T}\right)_{P,x} dT - \left(\frac{\partial \mu}{\partial P}\right)_{T,x} dP = 0,$$

$$d\mu_1 + x_2 d\mu_{21} + x_3 d\mu_{31} - \left(\frac{\partial \mu}{\partial T}\right)_{P,x} dT - \left(\frac{\partial \mu}{\partial P}\right)_{T,x} dP = 0,$$

where $d\mu_{21} = d\mu_2 - d\mu_1$.

Thus,

$$x_2 = -\left(\frac{\partial \mu_1}{\partial \mu_{21}}\right)_{T,P,\mu_{31}}, \qquad x_3 = -\left(\frac{\partial \mu_1}{\partial \mu_{31}}\right)_{T,P,\mu_{21}},$$

$$\rho = \left(\frac{\partial P}{\partial \mu_1}\right)_{T,\mu_{21},\mu_{31}}, \qquad S = -\left(\frac{\partial \mu_1}{\partial T}\right)_{P,\mu_{21},\mu_{31}}. \tag{3.7}$$

The variables are made dimensionless as:

$$\hat{\mu}_i = \frac{\mu_i}{k_B T_c}, \hat{\mu}_{ji} = \hat{\mu}_j - \hat{\mu}_i,$$

$$\hat{\rho} = \frac{\rho}{\rho_c}$$

$$\hat{S} = \frac{S}{k_B}.$$

Thus, dimensionlessly:

$$x_2 = -\left(\frac{\partial \hat{\mu}_1}{\partial \hat{\mu}_{21}} \right)_{T,P,\mu_{31}},$$

$$x_3 = -\left(\frac{\partial \hat{\mu}_1}{\partial \hat{\mu}_{31}} \right)_{T,P,\mu_{21}},$$

$$\hat{\rho} = \left(\frac{\partial \hat{P}}{\partial \hat{\mu}_1} \right)_{T,\mu_{21},\mu_{31}}, \tag{3.8}$$

$$\hat{S} = -\left(\frac{\partial \hat{\mu}_1}{\partial \hat{T}} \right)_{P,\mu_{21},\mu_{31}}.$$

Based on the expressions derived for the physical properties x_2, x_3, $\hat{\rho}$ and $\hat{S}$, expressions are now developed that relate these physical properties to the theoretical scaling densities. The relation between the scaling fields and the order parameters are given as: $dh_3 = \phi_1 dh_1 + \phi_2 dh_2$.[23] Substituting the value of h_1, h_2 and h_3 from Eq. (3.5), we get:

$$\begin{aligned} & d\left(c_1 \Delta \hat{P} + c_2 \Delta \hat{\mu}_1 + c_3 \Delta \hat{T} + c_4 \Delta \hat{\mu}_{21} + c_5 \Delta \hat{\mu}_{31} \right) = \\ & \phi_1 \;\; d\left(a_1 \Delta \hat{\mu}_1 + a_2 \Delta \hat{T} + a_3 \Delta \hat{P} + a_4 \Delta \hat{\mu}_{21} + a_5 \Delta \hat{\mu}_{31} \right) + \\ & \phi_2 \;\; d\left(b_1 \Delta \hat{T} + b_2 \Delta \hat{\mu}_1 + b_3 \Delta \hat{P} + b_4 \Delta \hat{\mu}_{21} + b_5 \Delta \hat{\mu}_{31} \right). \end{aligned} \tag{3.9}$$

Therefore, solving for x_2, x_3, $\hat{\rho}$ and $\hat{S}$ based on Eq. (3.9) the following expressions are obtained:

$$x_2 = -\left(\frac{\partial \hat{\mu}_1}{\partial \hat{\mu}_{21}}\right)_{T,P,\mu_{31}} = -\left(\frac{a_4\phi_1 + b_4\phi_2 - c_4}{c_2 - a_1\phi_1 - b_2\phi_2}\right), \tag{3.10}$$

$$x_3 = -\left(\frac{\partial \hat{\mu}_1}{\partial \hat{\mu}_{31}}\right)_{T,P,\mu_{21}} = -\left(\frac{a_5\phi_1 + b_5\phi_2 - c_5}{c_2 - a_1\phi_1 - b_2\phi_2}\right), \tag{3.11}$$

$$\hat{\rho} = \left(\frac{\partial \hat{P}}{\partial \hat{\mu}_1}\right)_{T,\mu_{21},\mu_{31}} = \left(\frac{a_1\phi_1 + b_2\phi_2 - c_2}{c_1 - a_3\phi_1 - b_3\phi_2}\right), \tag{3.12}$$

$$\hat{S} = -\left(\frac{\partial \hat{\mu}_1}{\partial \hat{T}}\right)_{P,\mu_{21},\mu_{31}} = \left(\frac{a_2\phi_1 + b_1\phi_2 - c_3}{c_2 - a_1\phi_1 - b_2\phi_2}\right). \tag{3.13}$$

Now the dependent scaling field h_3 is normalized and the coefficients within it are determined as follows:

From Eq. (3.6) the scaling field h_3 is given as: $h_3 = c_1\Delta\hat{P} + c_2\Delta\hat{\mu}_1 + c_3\Delta\hat{T} + c_4\Delta\hat{\mu}_{21} + c_5\Delta\hat{\mu}_{31}$

Making h_3 dimensionless, we obtain $c_1 = 1$.[23, 27]

At the critical point:

Density $\rho = \rho_c$ and $\phi_1 = \phi_2 = 0$. From Eq. (3.12) $\hat{\rho} = \frac{\rho}{\rho_c} = \left(\frac{-c_2}{c_1}\right) = 1$. This gives $c_2 = -1$.

Entropy $\hat{S} = \hat{S}_c$ and $\phi_1 = \phi_2 = 0$. From Eq.(3.13) $\hat{S} = \left(\frac{-c_3}{c_2}\right) = \hat{S}_c$. This gives $c_3 = \hat{S}_c$.

Composition $x_2 = x_{2c}$ and $\phi_1 = \phi_2 = 0$. From Eq. (3.10) $x_2 = \left(\frac{c_4}{c_2}\right) = -x_{2c}$.

This gives $c_4 = -x_{2c}$.

Composition $x_3 = x_{3c}$ and $\phi_1 = \phi_2 = 0$. From Eq. (3.11) $x_3 = \left(\frac{c_5}{c_2}\right) = -x_{3c}$.

This gives $c_5 = -x_{3c}$.

Hence the dependent scaling field is $h_3 = \Delta\hat{P} - \Delta\hat{\mu}_1 - \hat{S}_c\,\Delta\hat{T} - x_{2c}\Delta\hat{\mu}_{21} - x_{3c}\Delta\hat{\mu}_{31}$.

Substituting the above determined coefficients in Eqs. (3.10 – 3.13), we get:

$$x_2 = -\left(\frac{\phi_1 + b_4\phi_2 + x_{2c}}{-1 - a_1\phi_1 - b_2\phi_2}\right), \tag{3.14}$$

$$x_3 = -\left(\frac{a_5\phi_1 + b_5\phi_2 + x_{3c}}{-1 - a_1\phi_1 - b_2\phi_2}\right). \tag{3.15}$$

$$\hat{\rho} = \left(\frac{a_1\phi_1 + b_2\phi_2 + 1}{1 - a_3\phi_1 - b_3\phi_2}\right), \tag{3.16}$$

$$\hat{S} = \left(\frac{a_2\phi_1 + b_1\phi_2 + \hat{S}_c}{-1 + a_1\phi_1 + b_2\phi_2}\right). \tag{3.17}$$

These are the fundamental relations relating the physical variables and the theoretical variables. As seen above, in order to determine the concentration profiles, the unknown coefficients a_1, a_5, b_2, b_4 and b_5 need to be determined. Hence, one needs to accurately estimate the value of these coefficients from available experimental data. The coefficients a_1, b_2 and b_4 can be determined by using binary data alone, as shown by Wang et al.[23,27] The other two system-dependent coefficients, a_5 and b_5, depend on ternary data and lead to the asymmetric behavior of the system. In the following two sections, evaluation of these coefficients for a dilute ternary system is described. In the next chapter, the application of these equations to a real ternary system, methanol+cyclohexane+water is described.

3.7 Determination of coefficients from binary data

As shown by the work of Wang et al.,[23, 27, 28] the coefficients a_1, b_2 and b_4 can be estimated from binary data alone. It is shown that for a binary liquid mixture, the concentration of a solute ($x = x_2$) in the two coexisting phases, (x' and x'' in each phase respectively) has a temperature expansion as follows: [27]

$$\frac{x^{'} - x^{''}}{2x_c} = B_0 \left|\Delta T\right|^{\beta}, \tag{3.18}$$

$$\frac{x^{'} + x^{''}}{2x_c} = D_2 \left|\Delta T\right|^{2\beta} + D_1 \left|\Delta T\right|^{1-\alpha} + D_0 \left|\Delta T\right|, \tag{3.19}$$

where B_0, D_2, D_1 and D_0 are system dependent coefficients whose values are obtained by a least-squares fitting of the coexisting binary data and x_c is the critical composition of the solute. Hence these system dependent coefficients are related to the scaling coefficients a_1, b_2 and b_4 as follows:[27]

$$a_{eff} = \frac{D_2}{B_0^2}, \tag{3.20}$$

$$D_1 \left|\Delta T\right|^{1-\alpha} + D_0 \left|\Delta T\right| = -b_{eff} \left[\frac{A_0^-}{1-\alpha} \left|\Delta T\right|^{1-\alpha} - B_{cr} \left|\Delta T\right| \right], \tag{3.21}$$

where

$$a_{eff} = \frac{x_c a_1}{(1 - x_c a_1)}, \tag{3.22}$$

$$b_{eff} = \frac{(b_4 - x_c b_2)}{x_c (1 - S_c b_2)}. \tag{3.23}$$

In the above expressions A_0^- is the amplitude of the heat capacity, B_{cr} is the critical portion of the amplitude of the heat capacity, and S_c is the critical entropy. In the first approximation, it is assumed that $B_{cr} = \frac{1}{2} A_0^-$. In addition, it is observed that experimentally it is difficult to separate the coefficients b_4 and b_2.[27] Hence we can assume $b_2 = 0$.

Thus by using the above Eqs.(3.20 – 3.23), the binary scaling coefficients a_1, b_2 and b_4 can be determined. Further, to be able to determine the concentration profiles, the ternary coefficients a_5 and b_5 also need to be determined. These coefficients lead to the asymmetric behavior of the interface. In the following section, they are estimated based on ternary equilibrium data.

3.8 Determination of coefficients from ternary data

As derived in Eq. (3.15), the composition of the dilute species is given as: $x_3 = -\left(\frac{a_5\phi_1 + b_5\phi_2 + x_{3c}}{1 - a_1\phi_1 - b_2\phi_2} \right)$. In this section, determination of asymmetry coefficients a_5 and b_5 is described.

3.8.1 Determination of coefficient a_5:

From Eq. (3.6), the normalized scaling field h_1 is given as: $h_1 = \Delta\hat{\mu}_{21} + a_1\Delta\hat{\mu}_1 + a_2\Delta\hat{T} + a_3\Delta\hat{P} + a_5\Delta\hat{\mu}_{31}$. For an incompressible fluid, we can assume $\Delta\hat{P} = 0$. Hence the scaling field becomes, $h_1 = \Delta\hat{\mu}_{21} + a_1\Delta\hat{\mu}_1 + a_2\Delta\hat{T} + a_5\Delta\hat{\mu}_{31}$.

Along the critical locus $h_1 = 0$, hence we obtain: $-a_5 = a_1\frac{d\hat{\mu}_1}{d\hat{\mu}_{31}} + a_2\frac{d\hat{T}}{d\hat{\mu}_{31}} + \frac{d\hat{\mu}_{21}}{d\hat{\mu}_{31}}$.

Here $\frac{d\hat{\mu}_{31}}{d\hat{T}}$ is the entropy which can have an arbitrary value of zero. Hence $a_2 = 0$.

Thus, $-a_5 = a_1\frac{d\hat{\mu}_1}{d\hat{\mu}_{31}} + \frac{d\hat{\mu}_{21}}{d\hat{\mu}_{31}}$. (3.24)

Now, from thermodynamic relations:

$$d\mu_1 + x_2 d\mu_{21} + x_3 d\mu_{31} = 0,$$

$$\left(\frac{d\mu_1}{d\mu_{31}}\right)_{h_1=0} + x_{2c}\left(\frac{d\mu_{21}}{d\mu_{31}}\right)_{h_1=0} + x_{3c} = 0,$$

$$\left(\frac{d\mu_1}{d\mu_{31}}\right)_{h_1=0} = -x_{2c}\left(\frac{d\mu_{21}}{d\mu_{31}}\right)_{h_1=0} - x_{3c},$$

or dimensionleslsy,

$$\left(\frac{d\hat{\mu}_1}{d\hat{\mu}_{31}}\right)_{h_1=0} = -x_{2c}\left(\frac{d\hat{\mu}_{21}}{d\hat{\mu}_{31}}\right)_{h_1=0} - x_{3c}. \quad (3.25)$$

Substituting Eq. (3.25) into Eq. (3.24), we get:

$$-a_5 = a_1\left(-x_{2c}\left(\frac{d\hat{\mu}_{21}}{d\hat{\mu}_{31}}\right)_{h_1=0} - x_{3c}\right) + \frac{d\hat{\mu}_{21}}{d\hat{\mu}_{31}},$$

$$a_5 = a_1\left(x_{2c}\left(\frac{d\hat{\mu}_{21}}{d\hat{\mu}_{31}}\right)_{h_1=0} + x_{3c}\right) - \frac{d\hat{\mu}_{21}}{d\hat{\mu}_{31}},$$

$$a_5 = \frac{d\hat{\mu}_{21}}{d\hat{\mu}_{31}}\left(a_1 x_{2c} - 1\right) + a_1 x_{3c}. \tag{3.26}$$

Now the derivative $\frac{d\hat{\mu}_{21}}{d\hat{\mu}_{31}}$ is estimated as:

$$\frac{d\hat{\mu}_{21}}{d\hat{\mu}_{31}} = \frac{d\hat{\mu}_{21}}{dx_3}\frac{dx_3}{d\hat{\mu}_{31}} = K\left(\frac{dx_3}{d\hat{\mu}_{31}}\right),$$

where $K = \frac{d\hat{\mu}_{21}}{dx_3}$, (3.27)

is the Krichevskii parameter for a dilute three-component system.

In addition, for a dilute three-component system at the critical point,

$$\left(\frac{dx_3}{d\hat{\mu}_{31}}\right) = x_{3c}. \tag{3.28}$$

Hence $\frac{d\hat{\mu}_{21}}{d\hat{\mu}_{31}} = x_{3c}K.$ (3.29)

Substituting Eq. (3.29) in Eq. (3.26), the following expression for the asymmetry coefficient a_5 is obtained:

$$a_5 = x_{3c}\left[K\left(a_1 x_{2c} - 1\right) + a_1\right]. \tag{3.30}$$

3.8.2 Determination of coefficient b_5:

From Eq. (3.6), the normalized scaling field h_2 is given as:

$h_2 = \Delta\hat{T} + b_2\Delta\hat{\mu}_1 + b_3\Delta\hat{P} + b_4\Delta\hat{\mu}_{21} + b_5\Delta\hat{\mu}_{31}$. Along the path $h_2 = 0$, we obtain:

$$-b_5 = \left(\frac{d\hat{T}_c}{d\hat{\mu}_{31}}\right) + b_2\left(\frac{d\hat{\mu}_{1c}}{d\hat{\mu}_{31}}\right) + b_4\left(\frac{d\hat{\mu}_{21c}}{d\hat{\mu}_{31}}\right). \tag{3.31}$$

From the Gibbs-Duhem equation, and Eqs. (3.27) and (3.28), one obtains:

$$\left(\frac{d\hat{\mu}_1}{d\hat{\mu}_{31}}\right)_{h_1=0} = -x_{2c}\left(\frac{d\hat{\mu}_{21}}{d\hat{\mu}_{31}}\right)_{h_1=0} - x_{3c}, \quad \frac{d\hat{\mu}_{21}}{dx_3} = K, \quad \left(\frac{dx_3}{d\hat{\mu}_{31}}\right) = x_{3c},$$

and

$$\left(\frac{d\hat{T}_c}{d\hat{\mu}_{31}}\right)_{h_1=0} = \left(\frac{d\hat{T}_c}{dx_3}\frac{dx_3}{d\hat{\mu}_{31}}\right) = \frac{d\hat{T}_c}{dx_3}x_{3c}.$$

Substituting the above expressions in Eq. (3.31),one obtains:

$$-b_5 = \frac{d\hat{T}_c}{dx_3}x_{3c} + b_2\left(-x_{2c}\left(\frac{d\hat{\mu}_{21}}{d\hat{\mu}_{31}}\right)_{h_1=0} - x_{3c}\right) + b_4\left(\frac{d\hat{\mu}_{21c}}{d\hat{\mu}_{31}}\right),$$

$$-b_5 = \frac{d\hat{T}_c}{dx_3}x_{3c} + \frac{d\hat{\mu}_{21}}{d\hat{\mu}_{31}}\left(-x_{2c}b_2 + b_4\right) - x_{3c}b_2,$$

$$-b_5 = \frac{d\hat{T}_c}{dx_3}x_{3c} + \frac{d\hat{\mu}_{21}}{d\hat{\mu}_{31}}\left(-x_{2c}b_2 + b_4\right) - x_{3c}b_2,$$

$$-b_5 = \frac{d\hat{T}_c}{dx_3}x_{3c} + x_{3c}K\left(-x_{2c}b_2 + b_4\right) - x_{3c}b_2,$$

$$-b_5 = x_{3c}\left[\frac{d\hat{T}_c}{dx_3} + K\left(-x_{2c}b_2 + b_4\right) - b_2\right],$$

$$b_5 = -x_{3c}\left[\frac{d\hat{T}_c}{dx_3} + K\left(-x_{2c}b_2 + b_4\right) - b_2\right]. \tag{3.32}$$

Thus, Eqs. (3.30) and (3.32) are reasonable estimates for the asymmetry of the system. In addition to the ternary equilibrium data needed to evaluate these coefficients, there is another parameter which must be understood and evaluated. It is the Krichevskii parameter *K*.

3.9 Evaluation of the Krichevskii parameter

As defined above, the Krichevskii parameter for a dilute ternary system is expressed as: $K = \frac{d\,\hat{\mu}_{21}}{dx_3}$. It signifies the change in the amount of partial Gibbs energy within a binary system, on the addition of a third component. It is described further in this section.

The Gibbs energy for a binary system, by using the Margules approximation for excess energy is given as: $G = \frac{G^{\text{mix.}}}{RT} = x_1 \ln x_1 + x_2 \ln x_2 + A_{12} x_1 x_2$, where A_{12} is the binary-interaction parameter between species 1 and 2. If $x = x_2$, then

$$G = (1-x)\ln(1-x) + x\ln x + A_{12}x(1-x). \tag{3.33}$$

Now, evaluating *K*:

$$\hat{\mu}_{21} = \frac{\partial G}{\partial x} = \frac{\partial}{\partial x}\left[(1-x)\ln(1-x) + x\ln x + A_{12}x(1-x)\right],$$

$$\hat{\mu}_{21} = \ln x - \ln(1-x) + A_{12}(1-2x). \tag{3.34}$$

Hence,

$$K = \frac{d\,\hat{\mu}_{21}}{dx_3} = \frac{d}{dx_3}\left[\ln x - \ln(1-x) + A_{12}(1-2x)\right]$$

$$K = \frac{dx}{dx_3}\left[\frac{1}{x} + \frac{1}{1-x} - 2A_{12}\right] + (1-2x)\frac{dA_{12}}{dx_3} \tag{3.35}$$

where $x_2 = x_{2c}$.

For a dilute ternary system, the dependence of the third component on the binary-interaction parameter can be expressed as:

$$A_{12} = A_{12}^{0} + \frac{\partial A_{12}}{\partial x_3} x_3,$$

where A_{12}^{0} is the effect of only the binary interaction between species 1 and 2.

$$\therefore A_{12} = 2RT_c^{0} + x_3 \frac{d}{dx_3}\left(2RT_c\right),$$

$$A_{12} = 2RT_c^{0} + 2Rx_3 \frac{dT_c}{dx_3}.$$

Therefore, $\frac{dA_{12}}{dx_3} = 2R\frac{dT_c}{dx_3}$.

Making dimensionless by dividing by RT_c^{0}, we get

$$\frac{dA_{12}}{dx_3} = 2\frac{d\hat{T}_c}{dx_3}, \text{ where } \hat{T}_c = \frac{T_c}{T_c^{0}} \ . \tag{3.36}$$

Substituting Eq. (3.36) in Eq. (3.35), we get:

$$K = \left[\frac{1}{x_{2c}(1-x_{2c})} - 4 - 4x_{3c}\frac{d\hat{T}_c}{dx_3}\right]\frac{dx_2}{dx_3} + 2(1-2x_{2c})\frac{d\hat{T}_c}{dx_3}. \tag{3.37}$$

Thus the Krichevskii parameter for a dilute ternary system is evaluated as above.

In the following chapter, the concentration profiles for a real ternary system, methanol+cyclohexane+water, are determined by using the relations developed in this chapter.

Chapter 4: Methanol - Cyclohexane - Water System

4.1 Introduction

The previous two chapters dealt with modeling ternary systems and developing expressions to describe the interfacial concentrations of the components in a ternary system. In this chapter, the concentration profiles for a real ternary system, methanol-cyclohexane-water, are determined. The ternary system is analyzed to understand the effect of addition of a small amount of impurity into a binary system. Specifically, the effect of adding a small amount of water to a binary system of methanol-cyclohexane has been studied.

In this chapter, initially the methanol-cyclohexane-water ternary equilibria at standard conditions of temperature and pressure are presented. Then, the "pure" binary mixture of methanol-cyclohexane system is examined to evaluate the binary coefficients, as discussed in section 3.7. Following this, the effect of water on the phase behavior and the critical behavior of the methanol-cyclohexane system is presented. The data are then evaluated to determine the asymmetric coefficients in a ternary system, as discussed in section 3.8. Thus, with the help of this binary-ternary data and the relations developed in sections 3.6-3.9, the concentration profiles at the interface of the two-phase three-component system are plotted.

4.2 Methanol-cyclohexane-water ternary system under standard conditions

Based on the experimental data obtained from Plačkov and Štern,[2] the methanol–cyclohexane–water ternary system is plotted as shown in Fig. 4.1. In this paper, the experimental data have also been quantitatively verified by using certain semi-empirical models such as NRTL, UNIQUAC and the Bevia model.

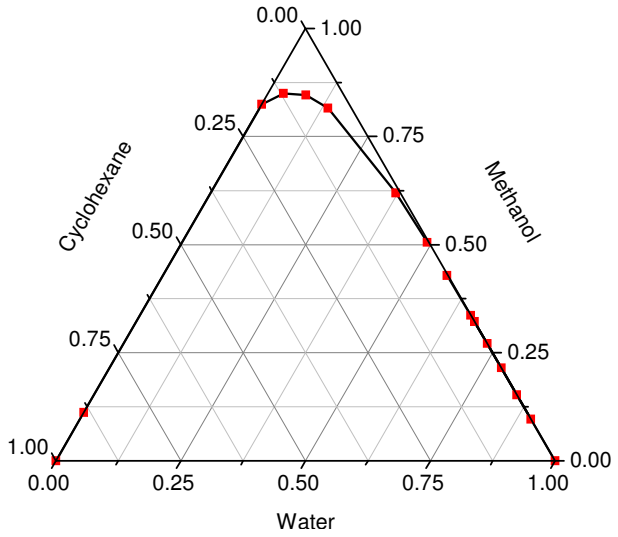

Fig. 4.1 Methanol-Cyclohexane-Water system at standard conditions [2]

In this thesis, the methanol-cyclohexane system with a dilute concentration of water is studied. The system studied constitutes a water concentration below 1%.

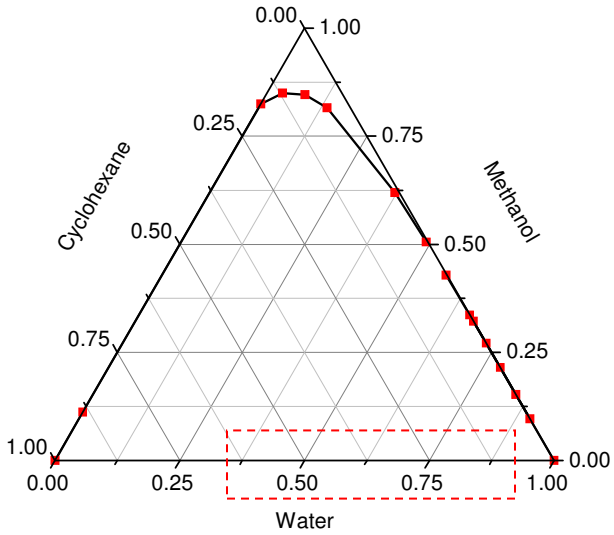

Fig. 4.2 Portion of Methanol-Cyclohexane-Water system studied in this thesis [2]

Thus the methodology involved in this study is to first understand the methanol–cyclohexane binary system. Then, the affect of adding a small amount of impurity in the form of water to this binary system is studied.

4.3 Methanol – Cyclohexane binary system

The methanol–cyclohexane binary system has been widely studied in literature.[2,5,6,24,29-37] Some of the published data show a slight discrepreancy,[5,6] and in this work the data published by *Ewing, Johnson and McGlashan* [5] will be referred to, because their paper includes detailed information on the methanol-cyclohexane binary system, which other papers do not.[6] The binary data from [5] are as shown below:

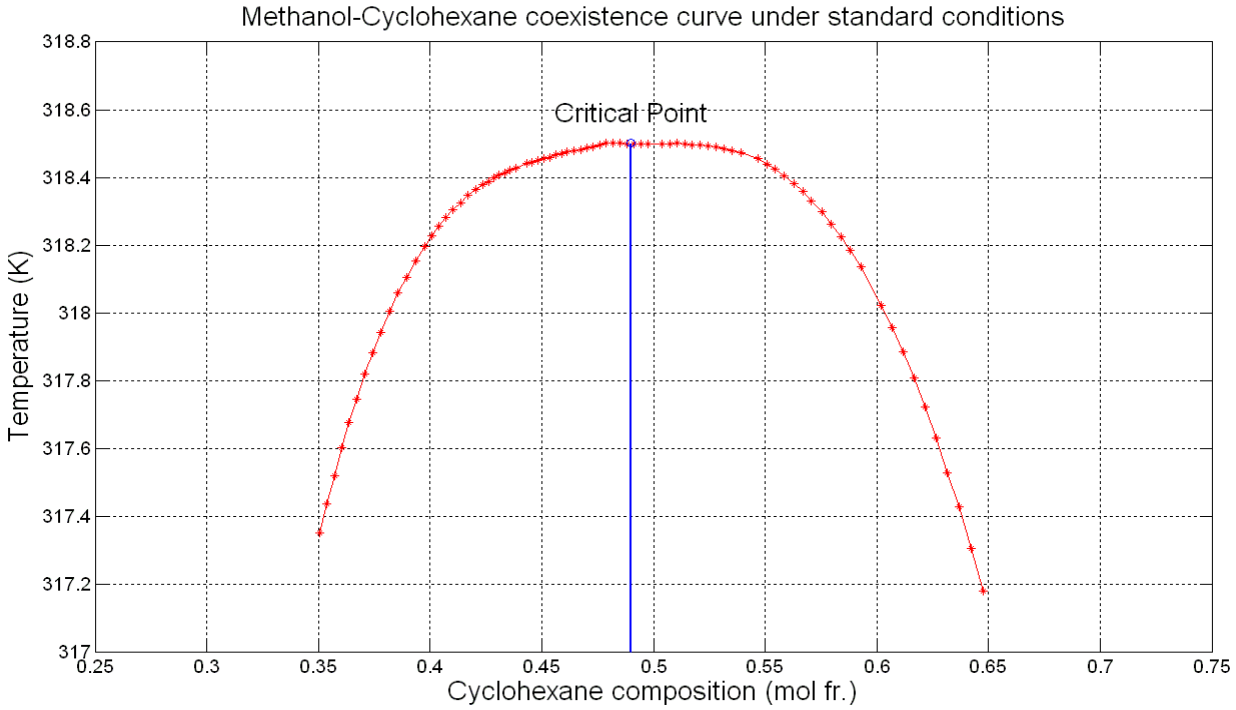

Fig. 4.3 Methanol-Cyclohexane binary system [5]

The critical parameters at a standard condition of 1atm pressure are: [2]

$T_c = 318.5$ K, (4.1)

$x_c = 0.490$, (4.2)

where x_c is the critical mole fraction of cyclohexane.

4.4 Analysis of methanol-cyclohexane binary data

As discussed in section 3.6, in order to determine the interfacial compositions, binary data are used to determine the coefficients a_1, b_2 and b_4. From the work of Wang and Anisimov,[27] the methanol-cyclohexane binary data can be represented as follows:

$$\frac{x' - x''}{2x_c} = B_0 \left|\Delta T\right|^{\beta}, \tag{4.3}$$

$$\frac{x' + x''}{2x_c} = D_2 \left|\Delta T\right|^{2\beta} + D_1 \left|\Delta T\right|^{1-\alpha} + D_0 \left|\Delta T\right|, \tag{4.4}$$

where x' and x'' are the mole fractions of cyclohexane in each of the two phases respectively. The critical composition of cyclohexane is $x_c = 0.49$, as given in Eq. (4.2), the distance from the critical point given as $\Delta T = \frac{T - T_c}{T_c}$, where $T_c = 318.5$ K as given in Eq. (4.1), and α and β are universal scaling constants given as 0.11 and 0.326 respectively. [38] The coefficients B_0, D_0, D_1 and D_2 are system dependent constants which are obtained by fitting the binary data into Eqs. (4.3) and (4.4). Due to the symmetric nature of the coexistence curve, the coefficient D_2 can be neglected.

The resultant binary data and the coefficients, fit into Eqs. (4.3) and (4.4) are as follows:

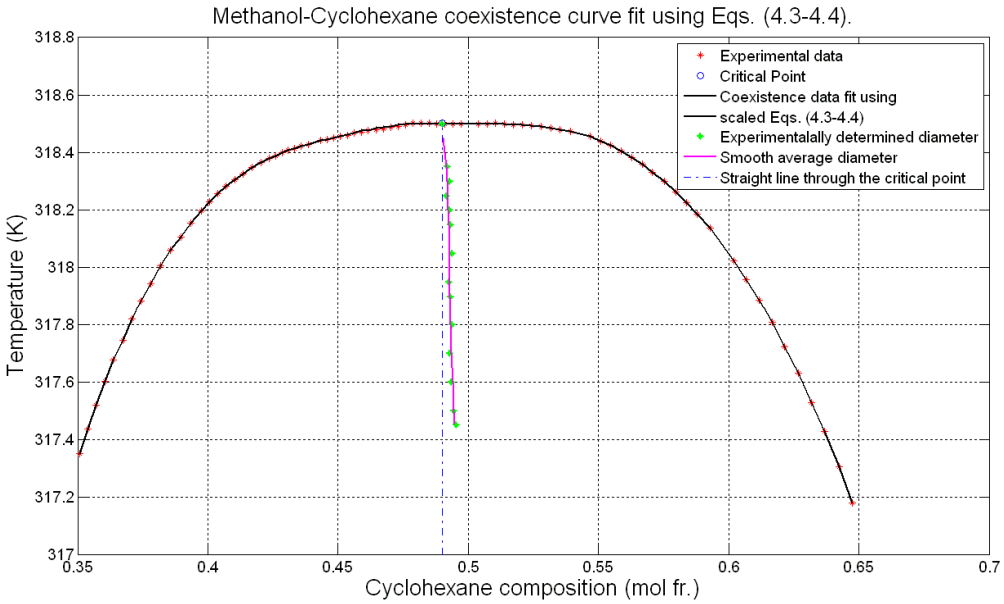

Fig. 4.4 Methanol-Cyclohexane binary data fit using Eqs. (4.3-4.4)

The resultant coefficients are evaluated by using the least squares fitting method and the estimated values are:

$B_0 = 1.853,$ (4.5)

$D_2 = 0.000,$ (4.6)

$D_1 = -0.057,$ (4.7)

$D_0 = 0.339.$ (4.8)

Thus, due to the symmetric nature of the binary curve, as seen in Fig. 4.1, only the coefficients D_1 and D_0 are fitted

The above derived constants are related to the system-dependent scaling coefficients as defined in Eqs. (3.22) and (3.23), as follows:

$$a_{\text{eff}} = \frac{D_2}{B_0^2}, \tag{4.9}$$

$$D_1 |\Delta T|^{1-\alpha} + D_0 |\Delta T| = -b_{\text{eff}} \left[\frac{A_0^-}{1-\alpha} |\Delta T|^{1-\alpha} - B_{\text{cr}} |\Delta T| \right], \tag{4.10}$$

where

$$a_{\text{eff}} = \frac{x_c a_1}{(1 - x_c a_1)}, \tag{4.11}$$

$$b_{\text{eff}} = \frac{(b_4 - x_c b_2)}{x_c (1 - S_c b_2)}. \tag{4.12}$$

In the above expression, A_0^- is the amplitude of the heat capacity at constant volume, estimated as 0.00147 J/cm^3 K[24, 37] where the universal ratio A_0^-/A_0^+ is taken as 0.523.[38] B_{cr} is the part of the isochoric heat capacity that arises due to fluctuations. In the first approximation, it can be assumed that $B_{\text{cr}} = \frac{1}{2} A_0^-$. In addition, the coefficients b_2 and b_4 being coupled,[27] it can be further assumed that $b_2 = 0$, and thus b_4 is determined from the above relations. The critical density of the binary system, needed to make A_0^- dimensionless is given as 0.7536 g/cc.[37]

The resulting system-dependent amplitudes are:

$A_0^- = 0.1362,$ (4.13)

$B_{\text{cr.}} = 0.0681.$ (4.14)

The resulting system-dependent binary coefficients are:

$a_1 = 0.0000,$ (4.15)

$b_2 = 0.0000,$ (4.16)

$b_4 = 0.0412.$ (4.17)

With these binary coefficients determined the next section deals with evaluation of ternary coefficients a_5 and b_5, which depend on the ternary phase behavior of the methanol-cyclohexane system with the addition of water.

4.5 Effect of addition of water

In section 3.8 of the previous chapter, expressions to determine the values of the system dependent coefficients a_5 and b_5, which depend on ternary equilibrium data, were developed. In this section, these coefficients are evaluated for methanol-cyclohexane-water system. Firstly, the equilibrium data on methanol-cyclohexane-water system from *Tveekrem and Jacobs*[39] are presented. The critical parameters needed to evaluate a_5 and b_5 are taken from this work.[39]

The following figure, Fig. 4.4, shows the methanol-cyclohexane coexistence curve on the addition of 0.45%, 0.65% and 0.85% of water. Comparing Fig. 4.4 with Fig. 4.3, one can distinctly see the difference in the nature of the phase diagram on the addition of water. Fig. 4.3 is quite symmetric, while Fig. 4.4 is highly asymmetric.

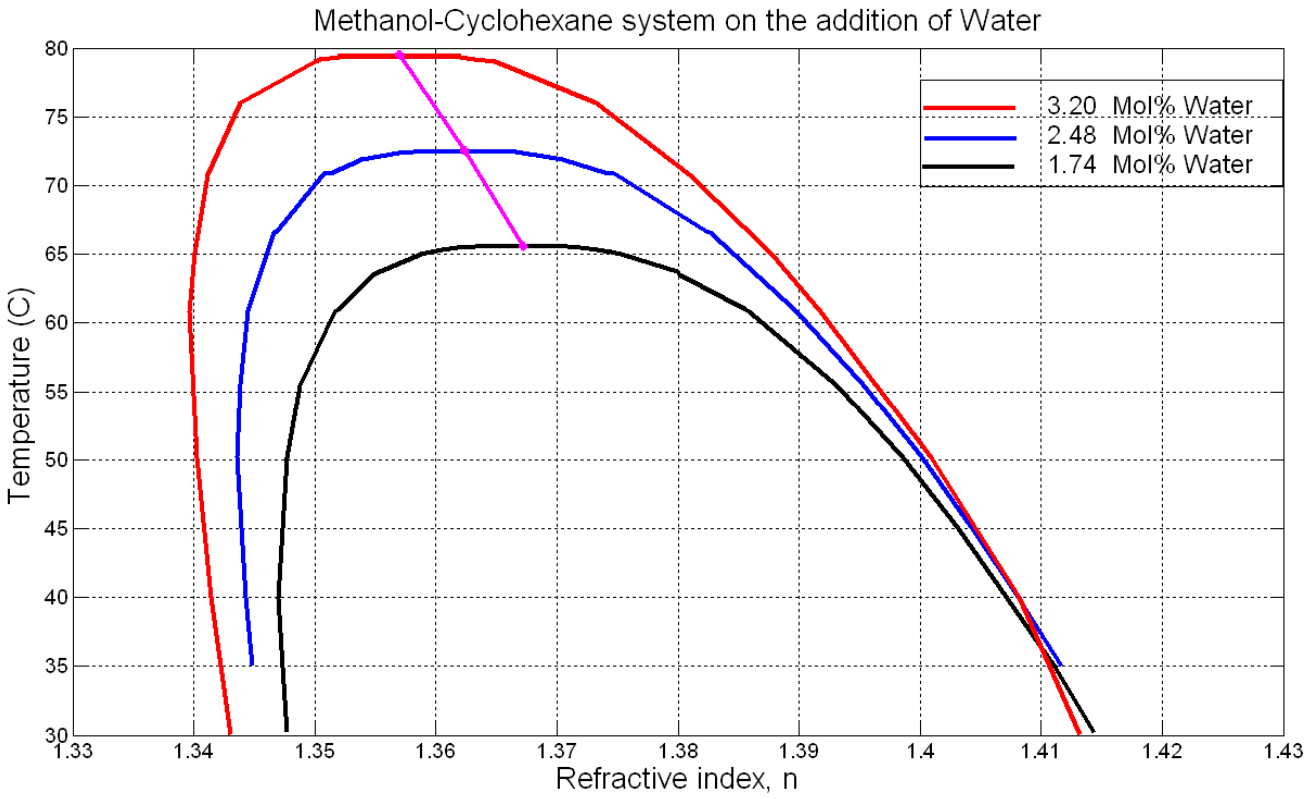

Fig. 4.5 Methanol-Cyclohexane coexistence curve upon the addition of water [39]

The following critical properties are obtained on analyzing the above coexistence curve: [39]

Methanol Composition (Vol %) x_{1c}	Cyclohexane Composition (Vol %) x_{2c}	Water Composition (Vol %) x_{3c}	Critical Temperature (K) T_c
31.9 %	67.65 %	0.45 %	338.75
32.3 %	67.05 %	0.65 %	345.64
33.1 %	66.05 %	0.85 %	352.62

Table 4.1. Critical properties of Methanol-Cyclohexane-Water system.

The other important critical parameters are:[39]

$$\frac{d\hat{T}_c}{dx_3} = 11.91,$$

$$\frac{dx_1}{dx_3} = 4,$$

$$\frac{dx_2}{dx_3} = -5,$$

where $d\hat{T}_c = d\left(\frac{T_c}{T_c^0}\right)$,

T_c : Critical temperature of dilute ternary system,

T_c^0 : Critical temperature of methanol-cyclohexane binary system.

The above values in mole fraction units are:

Compound Name	Methanol Composition (Mol %) x_{1c}	Cyclohexane Composition (Mol %) x_{2c}	Water Composition (Mol %) x_{3c}	Critical Temperature (K) T_c
Specific Gravity	**0.7918**	**0.779**	**1**	
Molecular Wt.	**32.04**	**84.16**	**18**	
	54.8 %	43.5 %	1.74 %	338.75
	54.9 %	42.6 %	2.48 %	345.64
	55.4%	41.4 %	3.20 %	352.62

$$\frac{d\hat{T}_c}{dx_3} = 3.059, \tag{4.18}$$

$$\frac{dx_1}{dx_3} = 1.7827, \tag{4.19}$$

$$\frac{dx_2}{dx_3} = -2.7827\ . \tag{4.20}$$

Substituting these values in Eqs. (3.30) and (3.32) for a_5 and b_5, we get:

$$a_5 = x_{3c}\left[K\left(a_1 x_{2c} - 1\right) + a_1\right], \tag{4.21}$$

$$b_5 = -x_{3c}\left[\frac{d\hat{T}_c}{dx_3} + K\left(-x_{2c}b_2 + b_4\right) - b_2\right], \tag{4.22}$$

where the Krichevskii parameter, K is determined from Eq. (3.37), as follows:

$$K = \left[\frac{1}{x_{2c}(1-x_{2c})} - 4 - 4x_{3c}\frac{d\hat{T}_c}{dx_3}\right]\frac{dx_2}{dx_3} + 2(1-2x_{2c})\frac{d\hat{T}_c}{dx_3}. \tag{4.23}$$

4.6 Revisiting order parameters

As discussed in section 3.6, the physical variables are expressed as:

$$x_2 = -\left(\frac{\phi_1 + b_4\phi_2 + x_{2c}}{1 - a_1\phi_1 - b_2\phi_2}\right), \tag{4.24}$$

$$x_3 = -\left(\frac{a_5\phi_1 + b_5\phi_2 + x_{3c}}{1 - a_1\phi_1 - b_2\phi_2}\right). \tag{4.25}$$

For the methanol-Cyclohexane-Water system, the binary and ternary coefficients are evaluated in the above sections 4.4 and 4.5. The order parameter ϕ_1 and ϕ_2 are to be evaluated now.

As discussed in section 3.3, the order parameter is a theoretical symmetrical variable that characterizes asymmetry in a system. The profile of the order parameter, or density of the lattice gas is as shown in the figure. A comparison between the mean-filed value and the one obtained from the following relation is made. An expression for the order parameter based on RG theory, obtained from Ohta and Kawasaki's work,[40] can be written as:

$$\phi_1 = \phi_{1,\pm\infty} \tanh\left(\frac{-z}{2\xi}\right)\left[1+\frac{2a}{3+a}\operatorname{sech}^2\left(\frac{-z\varepsilon}{2\xi}\right)\right]^{-1/2} \tag{4.26}$$

where

$$a = \frac{\sqrt{3}}{6}\pi\varepsilon, \tag{4.27}$$

$$\varepsilon = 4-d, \tag{4.28}$$

d = spatial dimensionality of the system (here: 3),

$$\phi_\infty = \pm B_0 \left|\Delta T\right|^\beta, \tag{4.29}$$

$$\xi = \xi_0^+ \left|\Delta T\right|^\nu . \tag{4.30}$$

$\xi_0^+ = 0.324$ nm

In the above expressions, ξ_0^+ is the amplitude of the correlation length above the critical point. It is of the order of a molecular size. It's order to equivalent to that of a molecular size. [11] The correlation length is half the width of the interface.[11,27]

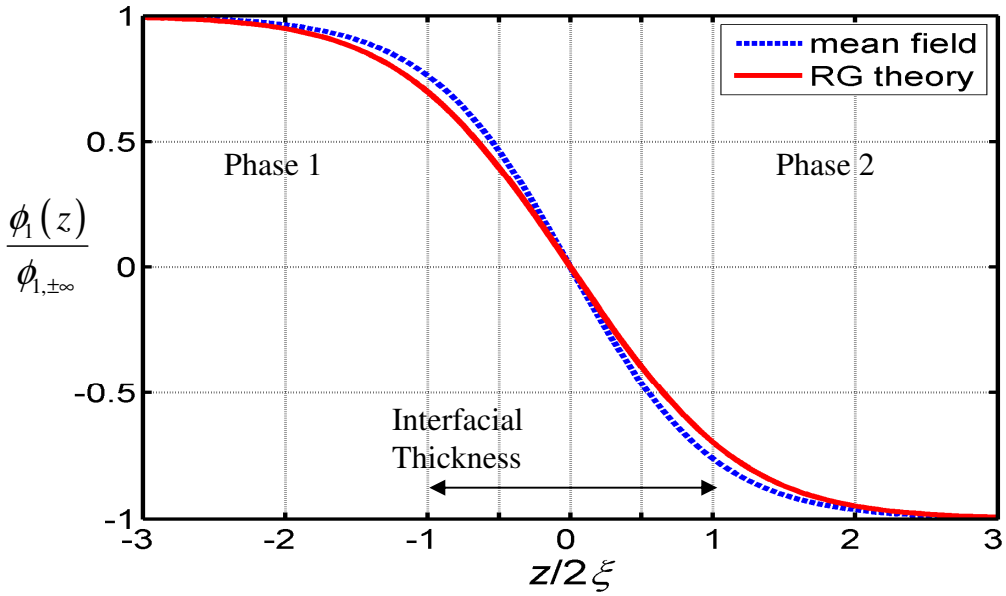

Fig. 4.6 Symmetric profile of the order parameter [46]

The second order parameter, the weakly fluctuating scaling density, is expressed as:[23]

$$\phi_2 \approx \frac{\hat{A}_0}{1-\alpha}\Delta\hat{T}\left|\Delta\hat{T}\right|^{-\alpha} + B_{\mathrm{cr}}\left|\Delta\hat{T}\right|, \tag{4.31}$$

where A_0^- is the amplitude of the isochoric heat capacity, as estimated in Eq. (4.13) in above section 4.4. However this expression is corrected in order to account for the entropy changes at the interfacial height (making it z-dependent). The modified weakly-fluctuating scaling density is given as follows. This is equivalent to the mean-field scaling density when $\xi = 0$.[41]

$$\varphi_2 = \left(\left[\frac{A_0^-}{1-\alpha}\right]\Delta\hat{T}\left|\Delta\hat{T}\right|^{-\alpha} + B_{cr.}\left|\Delta\hat{T}\right|\right)\left[\frac{\phi_1^2}{\phi_{1,\pm\infty}^2}\right]. \tag{4.32}$$

4.7 Temperature correction effects

Experimentally, the temperature in dilute systems is varied at a condition of constant concentration. However in the theoretical space, the scaling field h_2 is proportional to the temperature, which is varied at constant chemical potential, not concentration. i.e. $h_2 \propto \Delta\hat{T}_{\mu=\mu_c}$. Therefore a temperature correction is necessary. In dilute systems, the relation between the experimental temperature scale ($\Delta T(x)$: x-dependent) and the theoretical temperature scale ($\Delta T(\mu)$: μ–dependent) is a non-analytical function, and takes the following form:[42]

$$\frac{\Delta T(x)}{\tau_2} = \left[\frac{\Delta T(\mu)}{\tau_2}\right]^{1-\alpha}\left\{1+\frac{\Delta T(\mu)}{\tau_2}\right\}^{\alpha}, \tag{4.33}$$

$$\text{where } \tau_2 = \left[A_0^- x_{3c}(1-x_{3c})\left(\frac{d\hat{T}_c}{dx_3}\right)^2\right]^{1/\alpha}. \tag{4.34}$$

Thus the experimentally observed temperature scale is converted to the theoretical temperature scale and substituted in Eqs. (4.26) – (4.32), developed in above section 4.6 to determine the order parameter.

4.8 Plotting impurity concentration profiles

Based on the expressions developed in the above sections, the concentration profiles for water are plotted below. The relations used are described in the following table:

Relations	Derivation
$x_3 = -\left(\frac{a_5\phi_1 + b_5\phi_2 + x_{3c}}{1 - a_1\phi_1 - b_2\phi_2} \right)$	Eq. (4.25)
x_{3c}	From Table 4.1.
$a_5 = x_{3c}\left[K\left(a_1 x_{2c} - 1\right) + a_1 \right]$	Eq. (4.21)
$b_5 = -x_{3c}\left[\frac{d\hat{T}_c}{dx_3} + K(-x_{2c}b_2 + b_4) - b_2 \right]$	Eq. (4.22)
$K = \left[\frac{1}{x_{2c}(1-x_{2c})} - 4 - 4x_{3c}\frac{d\hat{T}_c}{dx_3} \right]\frac{dx_2}{dx_3} + 2(1-2x_{2c})\frac{d\hat{T}_c}{dx_3}.$	Eq. (4.23)
$a_1 = 0.0000$	Eq. (4.15)
$b_2 = 0.0000$	Eq. (4.16)
$b_4 = 0.0412$	Eq. (4.17)
$\frac{d\hat{T}_c}{dx_3} = 3.059$	Eq. (4.18)
$\frac{dx_1}{dx_3} = 1.7827$	Eq. (4.19)
$\frac{dx_2}{dx_3} = -2.7827$	Eq. (4.20)
$\phi_1 = \phi_{1,\pm\infty}\tanh\left(\frac{-z}{2\xi}\right)\left[1 + \frac{2a}{3+a}\sec h^2\left(\frac{-z\varepsilon}{2\xi}\right)\right]^{-1/2}$	Eq. (4.26)
$\phi_2 = \left(\left[\frac{A_0^-}{1-\alpha}\right]\Delta\hat{T}\left\|\Delta\hat{T}\right\|^{-\alpha} + B_{cr.}\left\|\Delta\hat{T}\right\|\right)\left[\frac{\phi_1^2}{\phi_{1,\pm\infty}^2}\right]$	Eq. (4.32)

Table 4.2: Relations used to determine impurity concentration profiles.

The concentration profiles are determined in two ways. In Fig. 4.5 and Fig. 4.6, the variation of concentration of water across the interface at two different critical concentrations 0.0248 and 0.0320 are plotted. They are at a constant distance of $d\hat{T}_c = \mathrm{dT} = 0.1$ from the critical temperature. As seen in the figure below, as the amount of impurity in the system increases, the interfacial profile becomes more asymmetric in nature. The amount of water in the heavier cyclohexane-rich phase ($z < 1$) is less compared to the amount of water in the lighter methanol-rich ($z > 1$) phase. This depicts the asymmetric nature of the system across the interface.

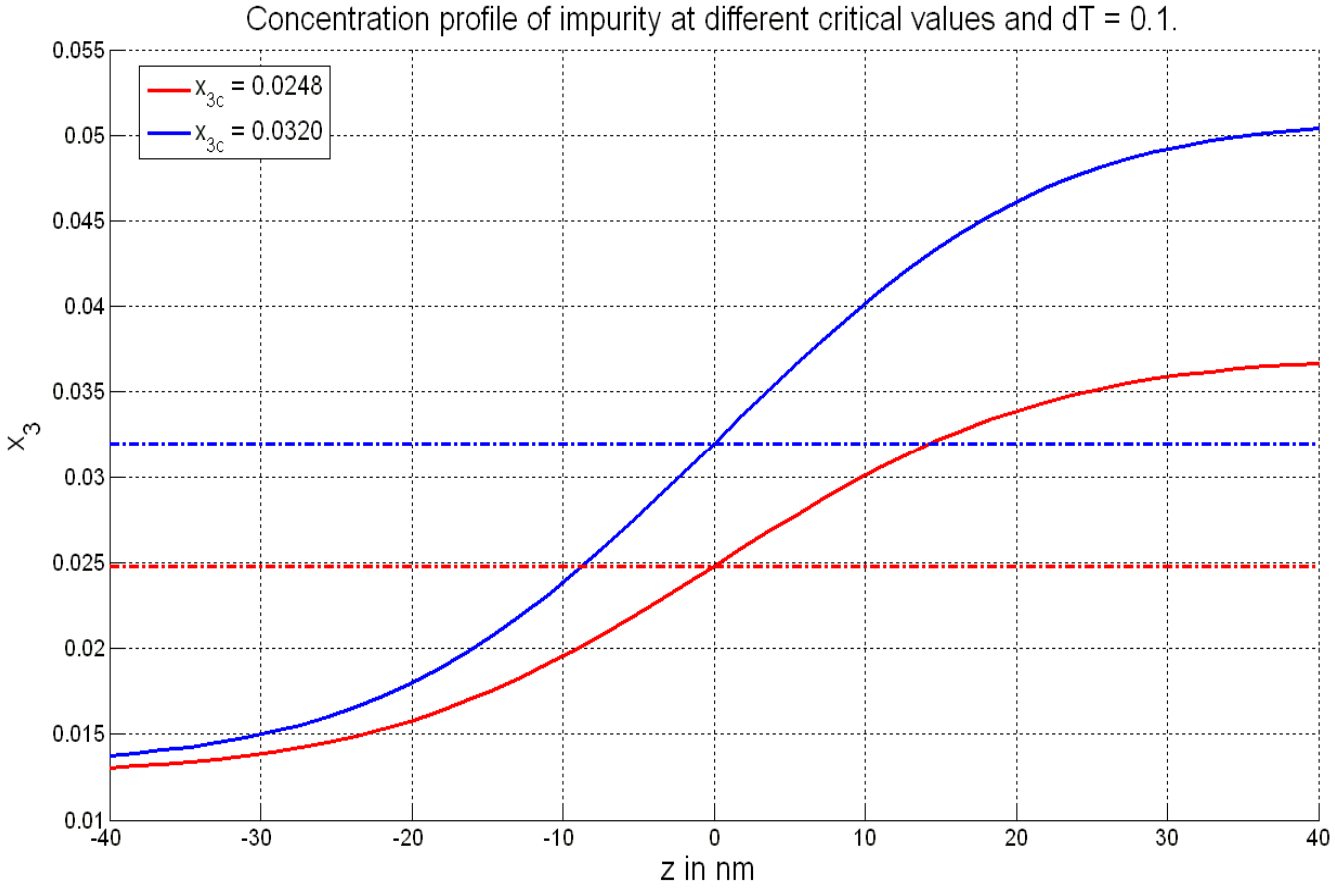

Fig. 4.7 Concentration profile of water at a fixed distance from the critical point, dT = 0.1.

The above figure can also be plotted as follows, depicting only the asymmetry. From Eq. (4.25), the only term that contributes to the asymmetry is the $b_5\phi_2$ term, the entropy term. Hence, this term is plotted as a function of z, as follows:

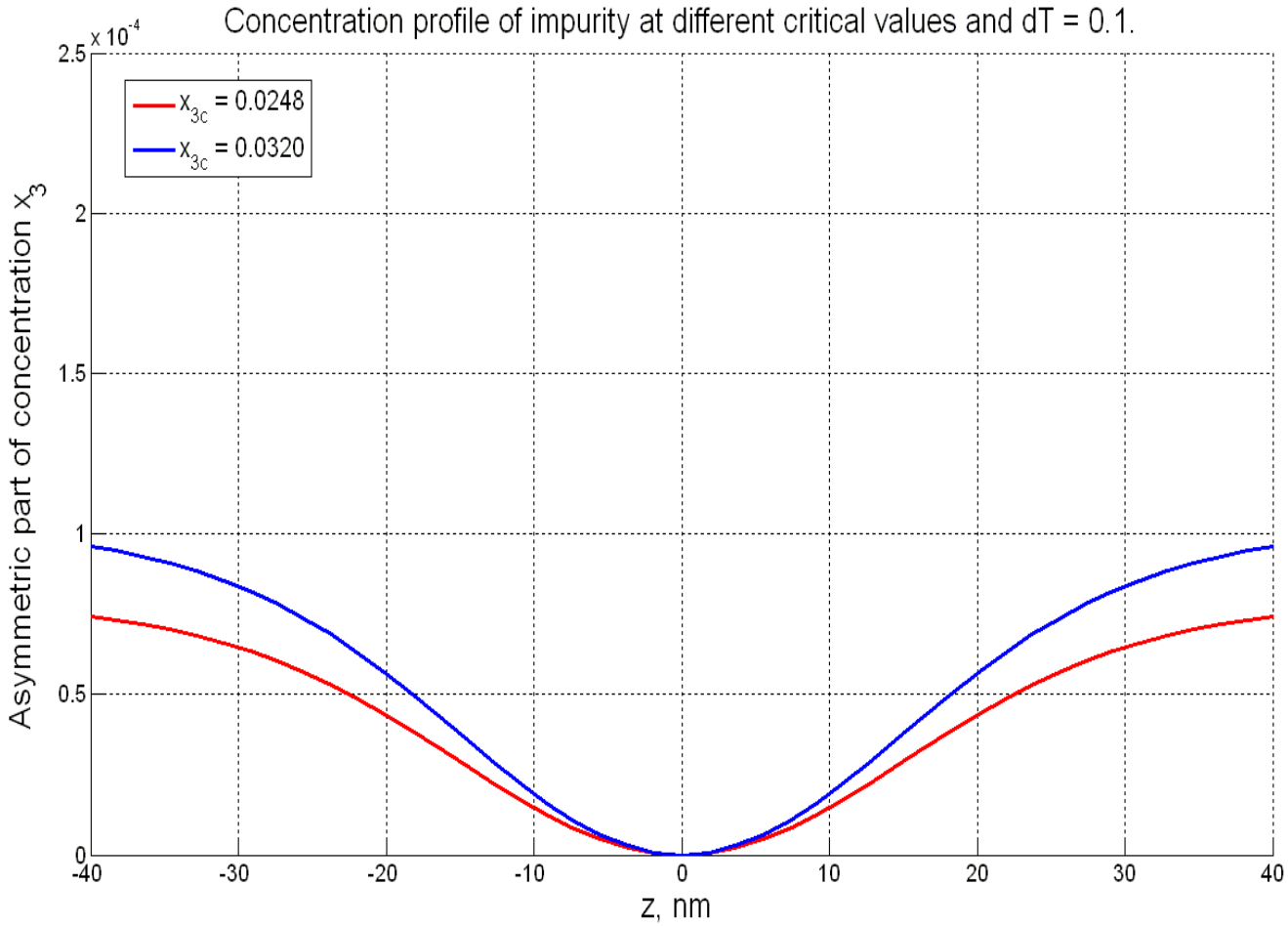

Fig. 4.8 Asymmetry in the concentration profile of water at a fixed distance from the critical point, dT = 0.1.

Another way to determine the concentration profiles is shown below. The concentration profiles are plotted at a fixed critical composition of x_{3c} = 0.0320, but at varying distances from the critical temperature, $d\hat{T}_c = dT$ = 0.01, 0.005, 0.001. As seen in Fig. 4.7 and Fig. 4.8 below, as one goes further away from the critical point, the system becomes more asymmetric in nature. Again the amount of water in the heavier cyclohexane-rich phase ($z < 1$) is less compared to the amount of water in the lighter methanol-rich ($z > 1$) phase. Thus the asymmetric nature of the interface is depicted and it is seen that the system approaches symmetry only asymptotically.

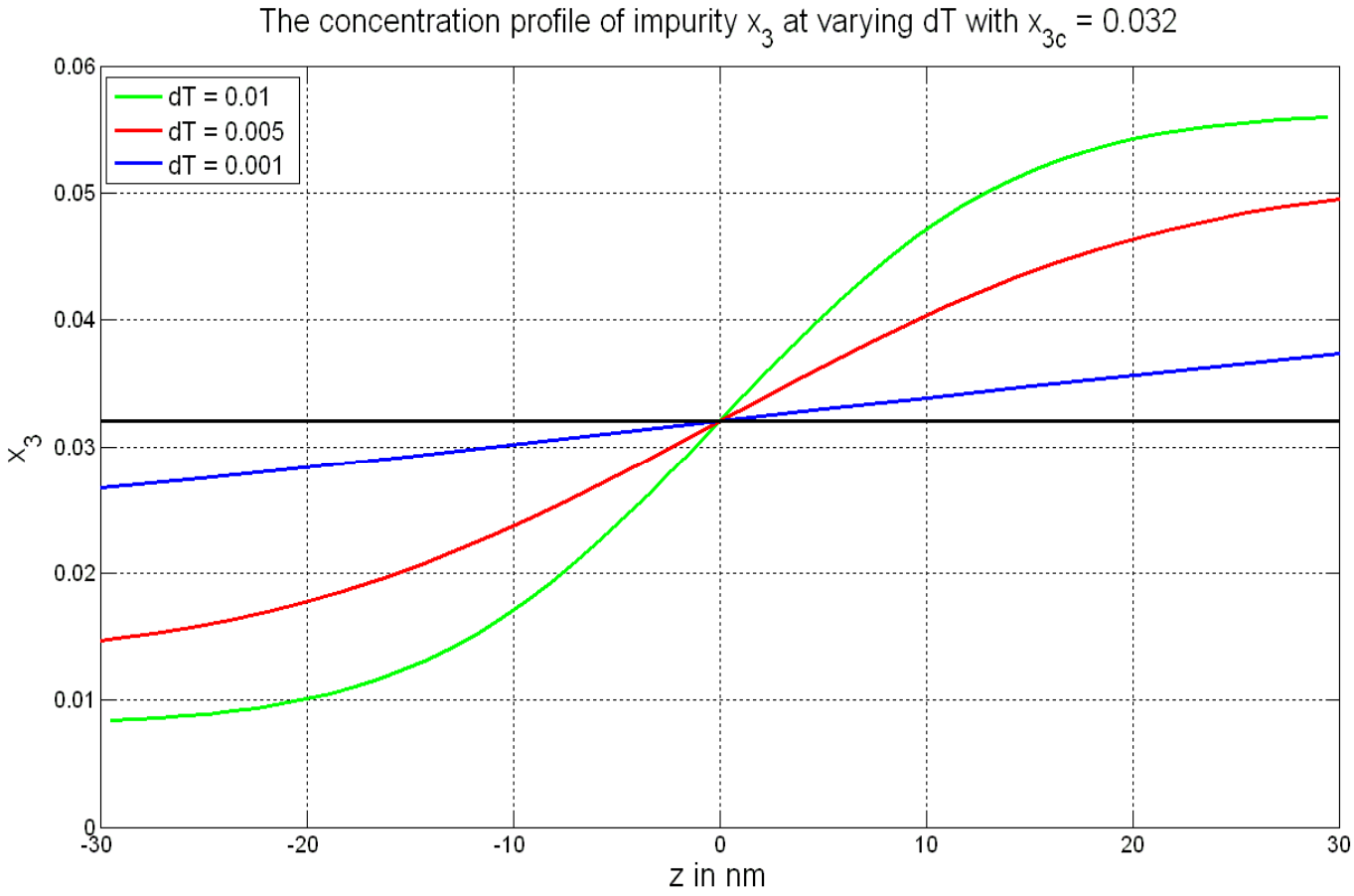

Fig. 4.9 Concentration profile of water at a fixed critical composition of x_{3c} = 0.032 and varying distances from the critical temperature.

In order to depict the asymmetry, only the asymmetric portion of Eq. (4.25) – the entropy term, is plotted as follows. It is clear from the following figure that as one approaches the critical temperature asymptotically, the system is symmetric and further away from the critical temperature, there is an asymmetric shift in the distribution of water between the methanol-rich and cyclohexane rich phases.

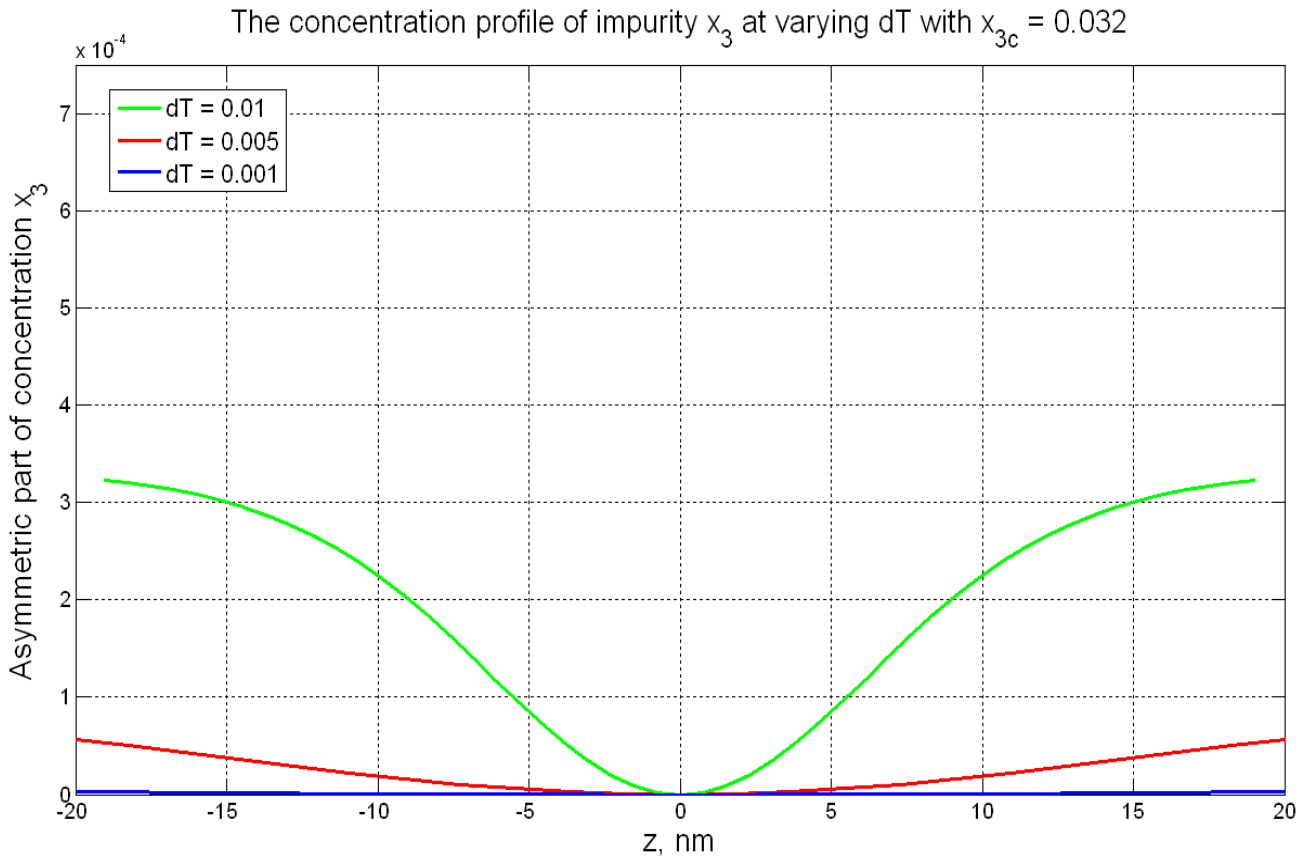

Fig. 4.10 Asymmetry in the concentration profile of water at a fixed critical composition of $x_{3c} = 0.032$ and varying distances from the critical temperature.

5. Conclusions and future work

In this research, interfacial concentration profiles for highly asymmetric, dilute ternary mixtures, using the symmetric order parameter from complete scaling, have been modeled. In addition, phase behavior in ternary systems was also analyzed.

Complete scaling was applied to ternary systems, by using the isomorphism principle. Based on the symmetric nature of the order parameter, a method was developed to determine the impurity concentration profiles in highly asymmetric ternary mixtures. The relations thus developed were applied to a dilute mixture of methanol-cyclohexane-water. It was observed that the distribution of the impurity across the interface was asymmetric. At a constant level of impurity concentration, as one moves further away from the critical temperature, the asymmetry in the interface increases. Moreover, at a constant distance from the critical temperature, as the impurity level in the system increases, the concentration profile becomes more asymmetric.

Thus the work done here provides a novel method to determine concentration profiles across interfaces in highly asymmetric ternary systems, by using the symmetric order parameter.

In a recent publication by *Japas et al*,[45] a method to estimate the Krichevskii parameter, as defined in section 3.3, Eq. (3.37) has been published. As discussed in section 3.3, this parameter describes the change in the free energy of a binary system on the addition of an impurity, or a third component. While the current research estimates the Krichevskii parameter based on a dilute regular solution approximation, the work of Japas et. al is based on molecular interactions between the species. Further work can be carried out to estimate the Krichevskii without any assumptions.

Another significant application of the current research would be to study micron sized liquid domains present in vesicles composed of ternary systems. It has been observed [43] that liquid domains within vesicles are most often circular in shape, but

when near the critical point they may become non-circular. It is also observed[43] that liquid domains in certain bilayers may fluctuate along their domain boundaries when near the critical points. These are two-dimensional systems and hence the fluctuations are large (micron scale). As seen in the following Fig. 5.1, near the critical point when the interfacial energy is small compared to the thermal energy, then the interface between the domains fluctuates.

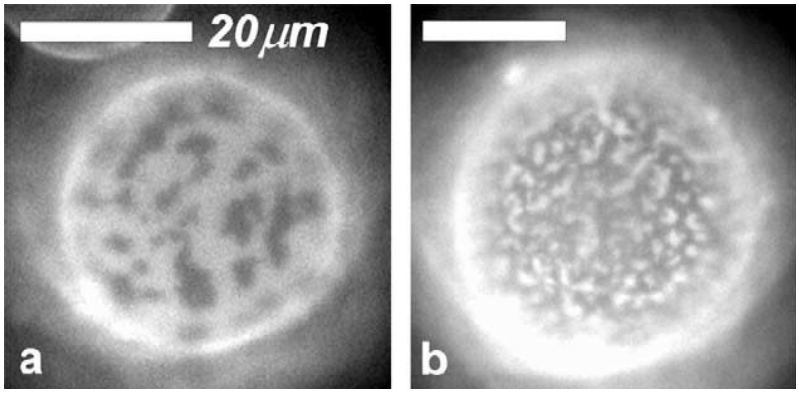

Fig. 5.1 Fluctuations observed at boundaries between liquid domains for compositions near critical point. [43] The system is Diphytanol phosphatidylcholine, Dipalmitoyl phosphatidylcholine and 50% Cholesterol.[43]

Fig. 5.1 a: At 20C Fig. 5.1 b: At 33C

As stated before, far away from the critical point the correlation length of fluctuations is the order of a molecule. This is also true for lipids in liquid phases.[43] Another phenomenon that occurs as you approach the critical point is that as the interfacial energy decreases, the line tension also decreases. The line tension which is found to be proportional to the size of the liquid domain,[44] or perimeter of the domain diverges when near the critical point.[43,44] Such behavior can be predicted by using scaling laws.

Appendix – Derivatives of G

$$G = x_1 \ln x_1 + x_2 \ln x_2 + x_3 \ln x_3 + A_{12} x_1 x_2 + A_{23} x_2 x_3 + A_{13} x_3 x_1$$

$$G_{11} = \frac{1}{x_1} + \frac{1}{x_3} - 2A_{13}$$

$$G_{12} = \frac{1}{x_3} + A_{12} - A_{23} - A_{13}$$

$$G_{22} = \frac{1}{x_2} + \frac{1}{x_3} - 2A_{23}$$

$$G_{111} = \frac{1}{x_3^2} - \frac{1}{x_1^2}$$

$$G_{112} = G_{122} = \frac{1}{x_3^2}$$

$$G_{222} = \frac{1}{x_3^2} - \frac{1}{x_2^2}$$

$$G_{1111} = \frac{2}{x_1^3} + \frac{2}{x_3^3}$$

$$G_{1112} = G_{1122} = G_{1222} = \frac{2}{x_3^2}$$

$$G_{2222} = \frac{2}{x_2^3} + \frac{2}{x_3^3}$$

$$\ln \boldsymbol{a}_1 = \ln x_1 + A_{12} x_2 (1 - x_1) + A_{13} x_3 (1 - x_1) - A_{23} x_2 x_3$$

$$\ln \boldsymbol{a}_2 = \ln x_2 + A_{12} x_1 (1 - x_2) - A_{13} x_1 x_3 + A_{23} x_3 (1 - x_2)$$

$$\ln \boldsymbol{a}_3 = \ln x_3 - A_{12} x_1 x_2 + A_{13} x_1 (1 - x_3) + A_{23} x_2 (1 - x_3)$$

References

1 R.E. Treybal, *Mass Transfer Operations*, McGraw Hill, 1980.

2 D. Plačkov and I. Štern, "Liquid-liquid equilibria for ternary systems of cyclohexane-water and C_1 to C_3 alcohols: data and predictions", *Fluid phase equilibria* **71**, 189 (1992).

3 J.M.Prausnitz, R.N. Lichtenthaler and E.G. de Azevedo, *Molecular thermodynamics of fluid-phase equilibria*, Prentice-Hall, 1986.

4 J.P. O'Connell and J.M.Haile, *Thermodynamics*, Cambridge, 2005.

5 M.B.Ewing, K.A.Johnson and M.L. McGlashan, "The liquid-liquid critical state of cyclohexane-methanol. IV. $(T, x)_p$ coexistence curve and the slope of the critical line", *J. Chem. Thermodynamics* **20**, 49 (1988).

6 A. Trejo, P. Yanez and R. Eustaquio-Rincon, "Liquid-liquid coexistence curves for binary systems: Methanol + Cyclohexane and + several isomers of Hexane", *J. Chem. Eng. Data* **51**, 1070 (2006).

7 R.V. Orye and J.M Prausnitz, "Multicomponent equilibria with the Wilson equation", *Ind. Eng. Chem*. **57**, 5 (1965).

8 M.A. Anisimov, *Lecture Notes in Thermodynamics* - ENCH 610 Fall 2007, University of Maryland, College Park.

9 M.M. Abott and J.M. Prausnitz, *Phase equilibria*, John Wiley & Sons, 1987. (retrieved from AIChE eLibrary).

10 J.P. Novak, J. Matous and J. Pick, *Liquid-liquid equilibria*, Elsevier Science, 1987.

11 M.A. Anisimov and H.J. St. Pierre, "Diverging curvature correction to the interfacial tension in polymer solutions," *Phys. Rev.* E **78**, 011105 (2008).

12 R. C. Tolman, "The effect of droplet size on surface tension", *J. Chem. Phys*. **17**, 333 (1949).

13 M.A. Anisimov, *Thermodynamics at the meso- and nano scale*, Dekker Encyclopedia of Nanoscience and Nanotechnology, 2004.

14 M. A. Anisimov, " Divergence of Tolman's length for a droplet neat the critical point", *Phys. Rev. Lett*. **98**, 035702 (2007).

15 J. M. Smith, H.C. Van Ness and M.M. Abott, *Chemical Engineering Thermodynamics*, McGraw Hill, 2003.

16 M. Góral, "Derivation of Wilson equation for G^E from association models", *Fluid-phase equilibria* **106**, 11 (1995).

17 A.W. Francis, *Liquid liquid equilibriums*, Interscience, 1963.

18 M. Gitterman, V. H. Halpern, *Phase transitions – A brief account with modern applications*, World Scientific, 2004.

19 J. Tolédano and P. Tolédano, *The Landau theory of phase transitions*, World Scientific, 1987.

20 C. Domb, *The critical point*, Taylor and Francis, 1996.

21 M.A. Anisimov, J.V. Sengers, *Equations of state for fluids and fluid mixtures*, IUPAC, Elsevier, Amsterdam, 2000.

22 Y.C. Kim, M.E. Fisher and G. Orkoulas, "Asymmetric fluid criticality. I. Scaling with pressure mixing," *Phys. Rev.* E **67**, 061506 (2003).

23 J. Wang and M.A. Anisimov, "Nature of vapor-liquid asymmetry in fluid criticality", *Phys. Rev.* E **75**, 051107 (2007).

24 M. A. Anisimov, *Critical phenomena in liquids and liquid crystals*, Gordon and breach, 1991.

25 M.A. Anisimov, E.E. Gorodetskii, V.D. Kulikov, J.V. Sengers, "Crossover between vapor-liquid and consolute critical phenomena", *Phys. Rev.* E **51**, 1199 (1995).

26 M. A. Anisimov, E.E. Gorodetskii, V.D. Kulikov, A. A. Povodyrev, J.V. Sengers, "A general isomorphism approach to thermodynamic and transport properties of binary fluid mixtures near critical points", *Physica* A **220**, 277 (1995); **223**, 272 (1996).

27 J. Wang, C. A. Cerdeirina, M.A. Anisimov, J.V. Sengers, "Principle of isomorphism and complete scaling for binary-fluid criticality", *Phys Rev.* E **77**, 031127 (2008).

28 M.A. Anisimov and J. Wang, "Nature of asymmetry in fluid criticality", *Phys. Rev. Lett*. **97**, 025703 (2006).

29 M.B.Ewing, K.A.Johnson and M.L. McGlashan, "The liquid-liquid critical state of cyclohexane-methanol. I. Excess molar enthalpies for $\{(1-x)c\text{-}C_6H_{12} + xCH_3OH\}$ within 1.3K of the critical temperature", *J. Chem. Thermodynamics* **17**, 513 (1985).

30 M.B.Ewing, K.A.Johnson and M.L. McGlashan, "The liquid-liquid critical state of cyclohexane-methanol. II. Use of the parametric equation of state to represent excess enthalpy in the critical region", *J. Chem. Thermodynamics* **18**, 979 (1986).

31 M.B.Ewing, K.A.Johnson and M.L. McGlashan, "The liquid-liquid critical state of cyclohexane-methanol. III. Excess molar volumes for $\{(1-x)c\text{-}C_6H_{12} + xCH_3OH\}$ at 14 temperatures within 2.4K of the critical temperature", *J. Chem. Thermodynamic*s **19**, 949 (1987).

32 M.B.Ewing, K.A.Johnson, "The liquid-liquid critical state of cyclohexane-methanol. V. Use of an asymmetric potential to represent excess volumes in the critical region", *J. Chem. Thermodynamics* **22**, 189 (1990).

33 D.T. Jacobs, "Critical point shifts in binary fluid mixtures", *J. Chem. Phys*. **91**, 560 (1989).

34 D.T. Jacobs, "Turbidity in the binary fluid mixture methanol-cyclehexane", *Phys. Rev*. A **33**, 2605 (1986).

35 R. Kopelman, R.W. Gammon, M.R.Molover, "Turbidity very near the critical point of methanol-cyclohexane mixtures", *Phys. Rev*. A **29**, 2048 (1984).

36 R. Behrends, U. Kaatze, M. Schach, "Scaling function of the critical binary mixture methanol-cyclohexane", *J. Chem. Phys.* **119**, 7957 (2003)

37 D.T. Jacobs, S.C. Greer, "Amplitude of the anomaly in the mass density near a liquid-liquid critical point", *Phys. Rev*. E **54**, 5358 (1996).

38 H. Behnejad, J.V. Sengers, M.A. Anisimov, *Thermodynamic behavior of fluids near critical points*.

39 J. L. Tveekrem, D. T. Jacobs, "Impurity effects in a near-critical binary-fluid mixture", *Phys. Rev*. A **27**, 2773 (1983).

40. T. Ohta, K. Kawasaki, "Renormalization group approach to the interfacial order parameter profile near the critical point", *Prog. Theor. Phys*. **58**, 467 (1977).

41 Obtained from work of C. Bertrand and M.A. Anisimov.

42 H. Cheng, M. A. Anisimov, J.V. Sengers, "Prediction of thermodynamic and transport properties in the one-phase region of methane and n-hexane mixtures, near their critical end points", *Fluid Phase Equi.* **128**, 67 (1997).

43 S.L Veatch, S.L. Keller, "Seeing spots: Complex phase behavior in simple membranes", *Biochimia et Biophysica acta*, **1746**, 172 (2005).

44 S.L. Keller, H.M. McConnell, "Stripe phases in lipid monolayers near a miscibility critical point", *Phys. Rev. Lett*. **82**, 1602 (1999).

45 K. I. Gutkowski, R. Fernandez-Prini, M. L. Japas, “Solubility of solids in near-critical conditions – Effect of a third component”, *J. Phys. Chem* B **112**, 5671 (2008).
46 H. St. Pierre, Ph.D. Proposal Defense, University of Maryland, College Park, 2008.